

1 **The 1538 eruption at Campi Flegrei resurgent caldera: implications for future unrest and**
2 **eruptive scenarios**

3 **Giuseppe Rolandi¹, Claudia Troise², Marco Sacchi³, Massimo di Lascio⁴, Giuseppe De Natale²**

4 ¹ Retired Professor at Università di Napoli Federico II, Dept. Earth Sciences, Naples (I)

5 ² Istituto Nazionale di Geofisica e Vulcanologia, Osservatorio Vesuviano, Naples (I)

6 ³ ISMAR-CNR, Naples (I)

7 ⁴ Free Lance Geologist, Naples (I)

8 Corresponding author: Giuseppe De Natale, giuseppe.denatale@ingv.it

9

10

11 **Abstract**

12 The recent unrest in the Campi Flegrei caldera which began several decades ago, poses a high risk to
13 a densely populated area, due to significant uplift, very shallow earthquakes of intermediate
14 magnitude and the potential for an eruption. Given the high population density, it is crucial, especially
15 for civil defense purposes, to consider realistic scenarios for the evolution of these phenomena,
16 particularly seismicity and potential eruptions. The eruption of 1538, the only historical eruption in
17 the area, provides a valuable basis for understanding how unrest episodes in this caldera may evolve
18 toward an eruption. In this paper, we provide a new historical reconstruction of the precursory
19 phenomena of the 1538 eruption, analyzed considering recent volcanological observations and results
20 obtained in the last few decades. This allows us to build a coherent picture of the mechanism and
21 possible evolution of the present unrest, including expected seismicity, ground uplift and eruptions.
22 Our work identifies two main alternative scenarios, providing a robust guideline for civil protection
23 measures, and facilitating the development of effective emergency plans in this highly risky area.

24 **1. Introduction**

25 The Campi Flegrei area has been a benchmark of modern geology and volcanology since the middle
26 XVIII century, due to the clear evidence of significant ground movements, associated with both uplift
27 and subsidence, imprinted on the columns of the ancient Roman Market (Macellum; hereafter also
28 called Serapeo) in the town of Pozzuoli. These movements were famously depicted on the cover of
29 Charles Lyell's 'Principles of Geology'. By the XIX century, it became evident that the impressive

relative movements between sea level and ground were due to ground uplift and subsidence. Consequently, numerous efforts have been made to reconstruct the timeline of these movements, during the centuries. One of the most convincing reconstructions was proposed by Parascandola (1947), later modified by Dvorak and Mastrolorenzo (1991), Morhange et al. (2006), Bellucci et al. (2006) and, most recently, Di Vito et al. (2016). These reconstructions, however, differ from each other. The ground movements have predominantly involved a long-term trend of subsidence, punctuated by occasional episodes of rapid uplift, culminating in the volcano's only historical eruption, in 1538 (Di Vito et al., 2016). After the 1538 eruption, a new period of subsidence began, which was interrupted in 1950, when a new series of uplift episodes commenced (Del Gaudio et al., 2010). Two major uplift episodes occurred between 1969-1972 and 1982-1984, characterized by rapid uplift (with a cumulative uplift of about 3.5 m) accompanied by seismicity: small in the first period, intense in the second one (with $M_{\max}=4.0$). These events led to the evacuation of 3000 residents from the oldest part of Pozzuoli town (Rione Terra), in 1970, and the entire town of Pozzuoli comprising 40.000 people, in 1984 (Barberi et al., 1984). After approximately 20 years of subsidence, a new uplift phase began in 2005-2006, with a much lower uplift rate (less than 0.01 meters per month on average, compared to about 0.06 meters per month in the 1970s and 1980s), but longer-lasting and still continuing at the time of writing. This new unrest has been accompanied by progressively increasing seismicity, which has substantially intensified, both in frequency and maximum magnitude (Troise et al., 2019; Kilburn et al., 2023; Iervolino et al., 2024). The maximum magnitude reached $M=4.6$ on March 13, 2025. The major increase in seismicity began when the maximum ground level attained at the end of 1984 was reached (in July 2022) and surpassed. The progressively increasing seismicity confirms the predictions of Kilburn et al. (2017) and Troise et al. (2019), who based their forecast on the correspondence of the ground level with stress levels at depth. This seismic activity represents a significant and continuous hazard for the edifices in such a densely populated area, given the very shallow depth of the earthquakes (about 2-3 km). Furthermore, the current crisis poses an even higher threat as it could potentially be a precursor to a future eruption in the area.

The present study primarily aimed to reconstruct and interpret the events before and after the 1538 eruption. This analysis follows three main paths: i) the accurate reconstruction, of the ground movements in this area since early historical times, using historical testimonies and documentation; ii) the accurate reconstruction of the uplift movements that evolved from 1430 to 1538, accompanied and followed by significant seismic events; iii) the analysis of stratigraphic and geophysical parameters, which, although collected in the recent era, provide important elements for the reconstruction and interpretation of the unrest related to the 1538 eruption.

63 Finally, the interpretation of the events preceding and following the 1538 eruption is used to provide
64 insight into possible evolution scenarios for the present unrest (Troise et al., 2019; Scarpa et al., 2022)
65

66 **2. Caldera formation and post-caldera volcanic activity 14 ka - 3.7 ka**

67 Campi Flegrei is an active caldera to the west of Naples in southern Italy. About 12-14 km
68 across, its southern third is submerged beneath the Bay of Pozzuoli. Following the most
69 recent, and likely only (Rolandi et al., 2020a; 2020b; De Natale et al., 2016), episode of
70 caldera formation, i.e. the Neapolitan Yellow Tuff eruption 15 ka, some 70 eruptions (linked
71 to 35 visible vents) have occurred across the caldera floor, ranging from the effusion of lava
72 domes to explosive hydro-magmatic eruptions (Di Vito et al., 1999; Smith et al., 2011; Isaia
73 et al., 2015). The most recent eruption occurred in 1538, producing the cone of Monte Nuovo
74 (Di Vito et al., 1987; 2016). Dome-shaped uplift of NYT occurred after the caldera formation
75 in the central zone of Campi Flegrei, with uplift up to hundreds of meters on the caldera floor
76 (Rolandi et al., 2020b). The significant uplift involved a large intra-calderic NYT block, making
77 Campi Flegrei a typical example of resurgent caldera (Luongo et al., 1991; Orsi et al., 1996; 1999;
78 Acocella (2010); Rolandi et al., 2020b). The post-caldera activity gave rise to numerous craters,
79 predominantly tuff cones and tuff rings (Fig. 1a,b), displaying the typical characters of
80 monogenic volcanoes (Marti et al., 2016). Within Campi Flegrei, 35 small eruptive centers
81 have been identified, since the NYT eruption (Di Vito et al., 1999; Smith et al., 2012),
82 producing about 70 eruptions. The magmas associated with these eruptions are typically
83 trachytes and alkali trachytes, with smaller amounts of latite and phonolite (Di Girolamo et
84 al., 1984; Rosi and Sbrana, 1987; D'Antonio et al., 1999). The post-caldera eruptions
85 can be then classified in two periods, occurring between 14 ka and 8.2 ka BP and 5.8 and
86 3.7 ka BP., respectively, with an interval of significant subsidence without eruptions
87 from 8.2 to 5.8 ka BP (Rolandi et al., 2020b).

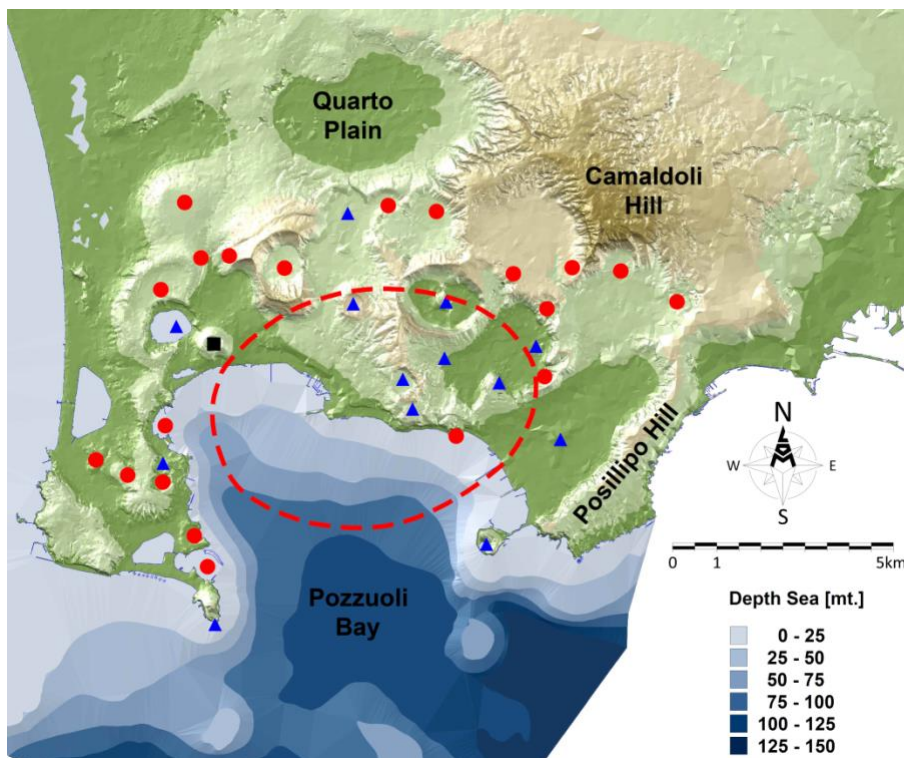
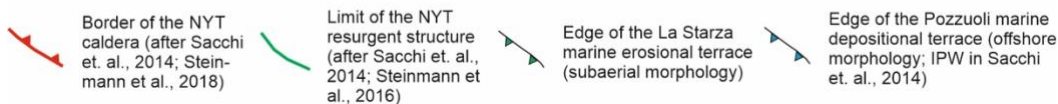
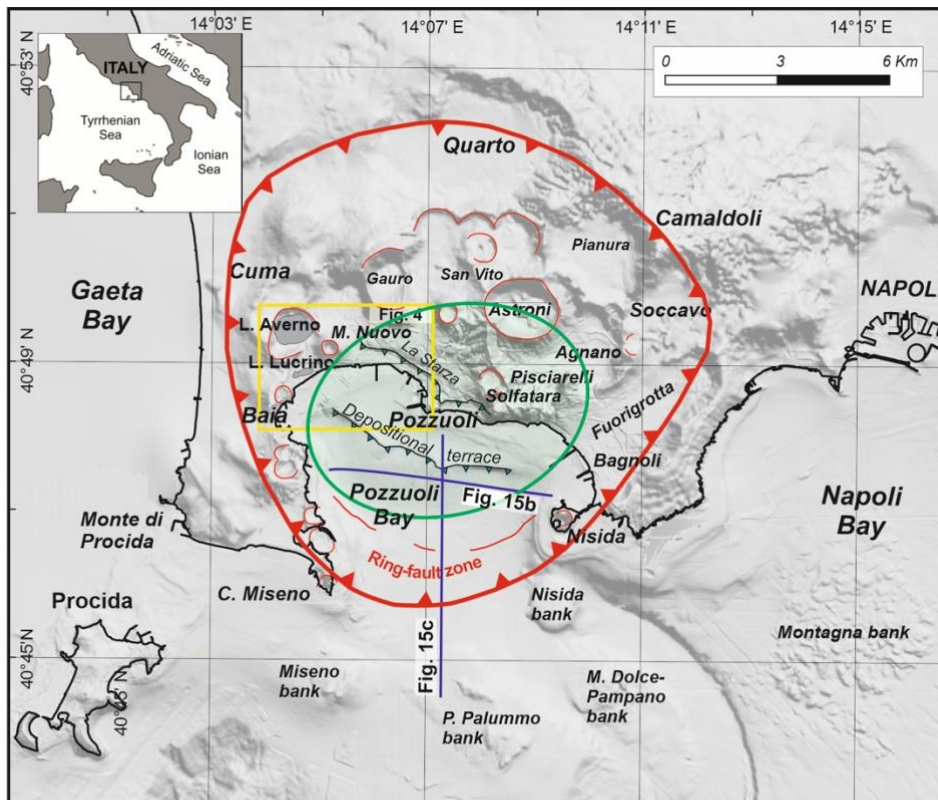


Fig. 1 – Top: Location map of the study area with indication of relevant toponyms and major volcano-tectonic and morpho-structural lineaments associated with the Campi Flegrei caldera. **Bottom:** Map of Campi Flegrei caldera. Red circles indicate the craters of the first post-caldera volcanic phase, blue triangles indicate the craters of the second phase. The red hatched area represents the resurgent block of NYT extended in the Pozzuoli Bay.

95

96 The second post-caldera eruptive phase was preceded by the uplift of 30m, above sea
97 level, of La Starza marine terrace (Cinque et al., 1983; Rolandi et al., 2020b). The
98 distribution of eruptive centers reveals that, during the first post-caldera phase, they were
99 distributed around the resurgent block. In the second phase, among thirteen volcanic edifices,
100 seven occurred within the resurgent area (Fig. 1).

101 It seems likely that the second post-caldera phase (5.8 - 3.7 ka) can be considered the primary
102 reference for defining possible future eruptive scenarios, following the eruption of 1538 AD.

103

104 **3. Subsidence and uplift evolution before the 1538 eruption**

105 **3.1 Previous interpretations**

106 Modern research on ground movements at Campi Flegrei caldera started with the detailed
107 studies by Parascandola (1943; 1947), the latter drawing mainly on earlier work by Niccolini
108 (1846). The 1943 study primarily focused on historical documents describing the
109 subsidence of the ancient Greek-Roman road known as ‘Via Herculea’, which was located
110 near the Averno volcano, and contributed to the formation of Lake Lucrino (Fig. 2).

111 The Via Herculea, in use since Greek times (beginning in the 8th century BC) and remaining
112 important throughout the Roman times, serves as fundamental historical marker for
113 assessing ground movements west of Pozzuoli. The detailed history of this road,
114 reconstructed from numerous historical sources and included in the supplementary material,
115 provides insights into its subsidence over the centuries.

116 The road ran along a narrow strip of land, probably formed by coastal aggradation of
117 volcanoclastic sandy deposits (Parascandola, 1943) primarily from the 5 ka and 3.7 ka
118 eruptions of the Averno and Capo Miseno volcanoes (Insinga et al., 2006; Di Vito et al.,
119 2011; Sacchi et al., 2014; Di Girolamo et al., 1984). The deposits eventually created a lake,
120 namely Lucrino (Fig. 2a). Given its elevation just a few meters above sea level, subsidence
121 significantly affected its usability, with frequent disruptions documented in historical
122 records. These records provide crucial evidence of the evolution of ground subsidence in
123 this area over the centuries.

124 The Greeks arriving from Euboea in the 8th century BC initially settled on the island of
125 Ischia (Pithecura), before founding the ‘polis’ of Cuma, the first Greek colony in Magna
126 Graecia and the entire western Mediterranean. Since these times the narrow land strip served
127 as a road known as the Via Herculea, providing access to the cultivated countryside around
128 Pozzuoli (Fig. 2b).

129 Parascandola (1943) emphasized the continuous subsidence of the Via Herculea, using
130 historical accounts from Petrarca (1341) and Boccaccio (1355-1373) to establish that the
131 road had already sunk below sea level by their time. He also noted that Via Herculea did not
132 re-emerge during the uplift accompanying the 1538 eruption, suggesting that the ground
133 uplift in this area was insufficient to compensate for the secular subsidence.
134 In his later work, Parascandola (1947) presented a detailed reconstruction of ground
135 movements in Pozzuoli, which has provided a common starting point for subsequent studies
136 on this subject. According to Parascandola (1947) the maximum subsidence occurred during
137 the IX century.
138 The first paper to propose an alternative model for ground movements at Campi Flegrei was
139 published by Dvorak and Mastrolorenzo (1991). They propose simplified and constant rates
140 of subsidence and uplift, suggesting that the maximum subsidence occurred at the end of
141 15th century.
142 Morhange et al. (1999; 2006), based on radiocarbon dating of bivalve shells, identified an
143 additional episode of ground uplift between 650 and 800 AD. Bellucci et al. (2006) later
144 integrated the ground deformation model of Dvorak and Mastrolorenzo (1991) with the
145 findings of Morhange et al. (1999; 2006) into a unified framework.
146 More recently, Di Vito et al. (2016) proposed a new reconstruction of ground movements,
147 which will be discussed in more detail below. Their model suggests that the maximum
148 subsidence occurred in 1251 AD. They also proposed that subsidence at Campi Flegrei began
149 around 35 BC, and that the ground at the Monte Nuovo vent uplifted by approximately 19
150 meters immediately before the 1538 eruption. The main reason of such different
151 interpretations was the use of only partial data sets.

152

153 **3.2 Reconstructing the ground movements with the whole available data set**

154 The inclusion of new historical documents allowed us to precisely reconstruct ground movements in
155 Pozzuoli area (central part of the caldera) and in the Averno area (3 km west of Pozzuoli, close to the
156 area where the 1538 eruption occurred. The reconstruction reported here, based on all the reliable
157 historical documents, hence allows to tightly constrain past ground movements, so resolving the
158 differences in previous interpretations.

159 The first evidence of subsidence in the Campi Flegrei area dates back Greek times, as reported by
160 Diodoro Siculo (VIII century BC) and is related to the area in front of the Averno Lake, close to the
161 vent of the 1538 eruption, which generated the Monte Nuovo cone. We will start to describe the

162 historical documents to shed light on the ground movements in this area, then we will reconstruct
163 ground movements in the most deformed, central Pozzuoli area.

164

165

166 3.2.1 Ground movements at Averno

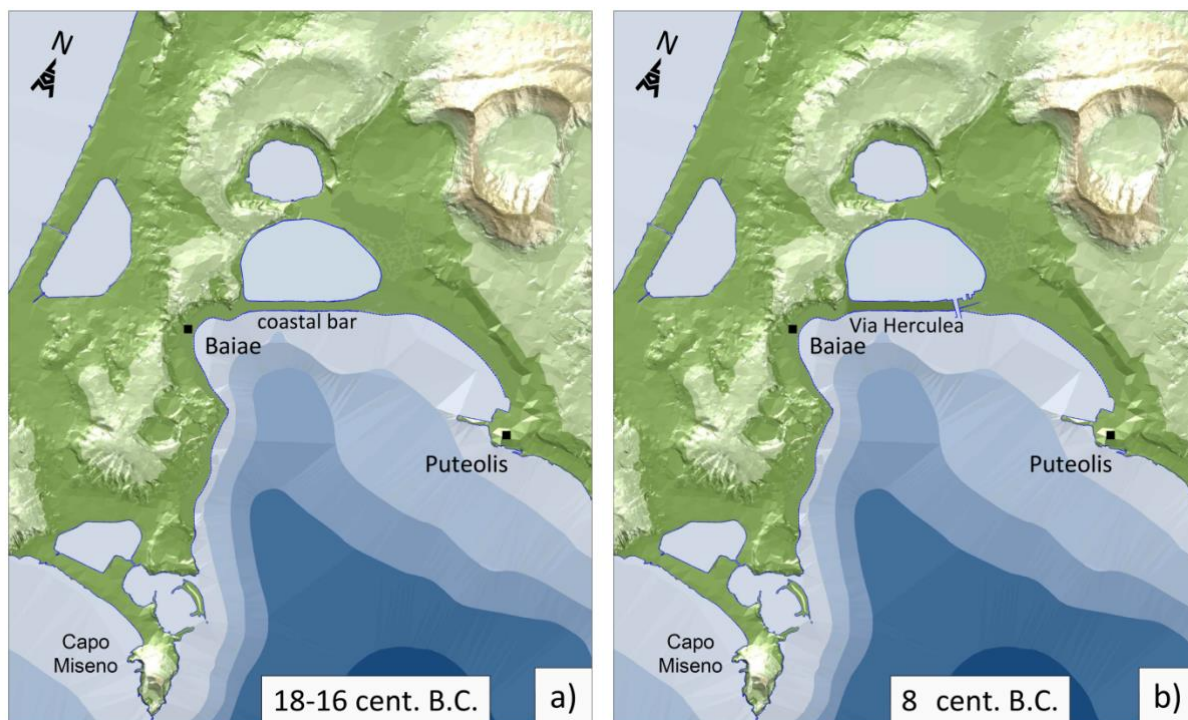
167

168 A fundamental historical marker for inferring the ground movements west of Pozzuoli, as already
169 mentioned, is the Via Herculea. Diodoro Siculo (see Appendix 1) reported that, already at the times
170 of first Greek settlements, i.e. 8th century BC, continuous subsidence affected this area, thus
171 generating problems to the practicability of Via Herculea.

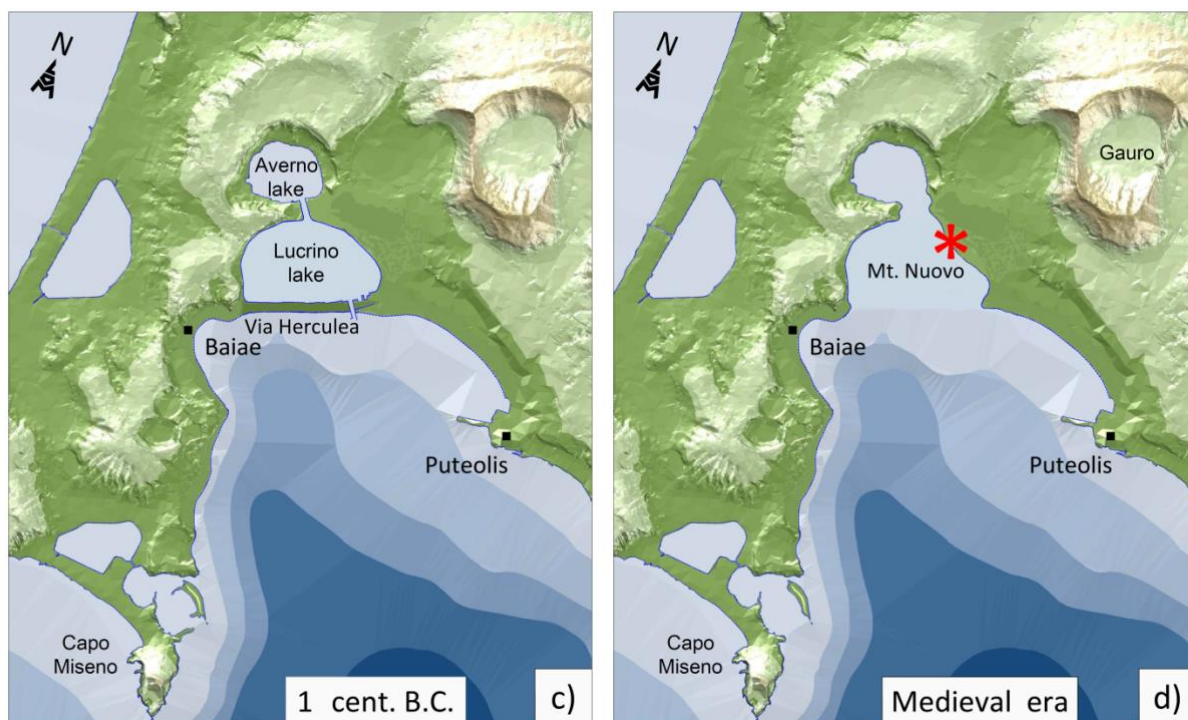
172 In Roman times, since the beginning of the 1st century BC, the body of water enclosed by the Via
173 Herculea, purchased by Sergio Orata, played an important role in fish-farming since 90 BC, taking
174 the name of Lucrino (from the latin term ‘lucrum’ for profit), much larger than the present-day Lake
175 Lucrino. After his death, continuous subsidence menaced both the practicability of the Via Herculea
176 and the fish farming activities. The new owners around 50 BC turned to the Roman Senate calling
177 for appropriate interventions. For this purpose, in the period 48-44 BC Julius Caesar was
178 commissioned, then building a barrier (*Opus Pilarum*) and special shutters to protect the road and the
179 Lucrino Lake from sea ingression (see Appendix 1). Towards the end of the same century, for military
180 purposes, in 37 BC Agrippa cut both the Via Herculea and the barrier with the crater of Avernus.
181 Having understood, unlike Julius Caesar, the continuous subsidence of the Via Herculea, which at
182 the end of the century was only few meters above sea level (Fig. 2c), Agrippa also **increased its**
183 **height** (Strabo, 1st century BC). About four centuries later, Theodoric (King of the Ostrogoths), upon
184 request for the protection of fish farming, restored the dam by increasing again the height of via
185 Herculea with respect to the sea level (Parascandola, 1943).

186 The Via Herculea finally sank below the sea level between 6th - 7th century A.D, when the sea
187 penetrated the crater of Averno, the Lake Lucrino having disappeared (Fig. 2d). Proof of the
188 disappearance of the Via Herculea and of the Lucrino Lake was also testified by Boccaccio, who
189 lived in the Naples area from 1327 to 1341 AD and described the Averno area in its geographical
190 book ‘De montibus’ (...to Avernus, connected in ancient times with the nearby lake Lucrino where it
191 recalls the waters of portus Iulius).

192



193



194

195

196

197

198

199

Fig. 2 - a,b,c,d) position and shape of the via Herculea, Lucrino and Averno lakes, along 33 centuries. The red star indicates the central point around which the volcanic edifice of 1538 was formed.

Via Herculea never rose above the sea level again, despite the large uplift phase occurred before and during the 1538 eruption (see Fig. 2d).

Our reconstruction of the level of Via Herculea, from the 8th century till 1538, is shown in Figs. 2 and 3. At the end of the 1st century BC and 4th century AD, works were carried out to increase the height of the route above sea level due to the incipient submersion. Due to these works, the submersion of the route was delayed from about the 3rd century AD, until the 7th century AD (Fig. 3). A date of submersion around 6-7th century is consistent with the observations by Parascandola (1943) that the Via Herculea was above sea level for much of the 6th century. The Via Herculea has remained submerged ever since (even during the 1538 eruption: Parascandola, 1943), and relics can be seen today about 4.5 meters bsl (Fig. 4). The submerged relicts of the Via Herculea are still visible today, located at about 4.5 meters bsl, as shown in the high-resolution bathymetry (Fig.4: Somma et al., 2016).

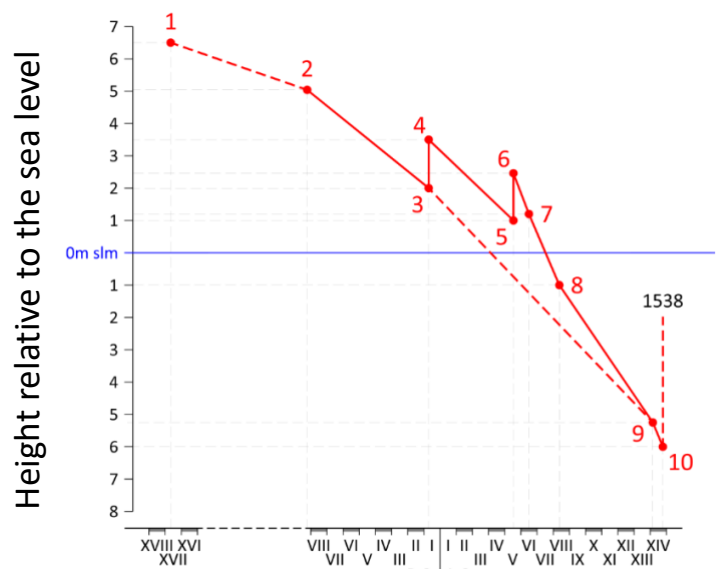


Fig. 3 – Diagram showing the trend of ground movements at the Via Herculea, as referred to sea level, along 33 centuries. Each point on the curve refers to a specific documented historical period, whose number indicates the reference for the inferred level. References are synthetically reported in Table 1 and extensively explained in Appendix 1. Dashed lines represent hypothesized subsidences: the first one connecting to the likely initial elevation, the second one showing the likely subsidence path in absence of the restoration works (points 4 and 6), the third one showing the likely uplift linked to 1538 eruption.

Number	Time	Event	Reference source	Reported by
1	3.7 ka and after	Formation of the coastal bar	This paper	
2	8 th century BC	Subsidence of the via Herculea	Diodorus Siculus (Book IV)	Parascandola, 1943
3	60 BC	Sergio Orata, owner of the ‘Lucrino’ lake fish farm, asked the Senate to have via Herculea repaired, because at	Parascandola, 1943	

		around 2 m asl. Cesare repaired it		
4	37 BC	Agrippa raised the level of via Herculea	Strabone	Parascandola, 1943
5	12 BC	Abandonment of Portus Julius and Lucrino fish farming, because of accelerated subsidence of via Herculea	Aucelli, 2020	
6	496 AD	Theodoric, King of Gotes, repaired and raised level of via Herculea	Cassiodorus, Varia Book I	Parascandola, 1943
7-8	556 AD	Failed attempts to restore fish farming in the Lucrino lake: the level of Dam was too low	Parascandola, 1943	
9	1341-1348	Petrarca and Boccaccio writings indicate via Herculea was about 5-6 m bsl	Boccaccio, 1355-1373	Parascandola, 1943
10	15 th century	Uplift starts, but Lucrino lake however disappeared and via Herculea never re-emerged	Several chroniclers of the time	Parascandola, 1943

Table 1 - Synthetic sketch of the main historical sources used to reconstruct the ground deformations shown in Fig.3 (see Appendix 1 for more details).

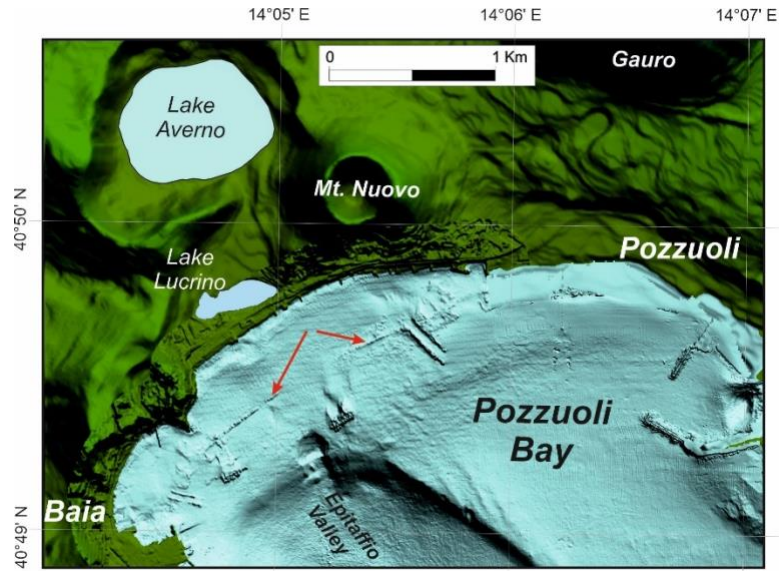


Fig. 4 – Shaded relief map of the coastal area of the Pozzuoli Bay based on high resolution multibeam bathymetry (Somma et al., 2016). Arrows indicate the submerged remains of the breakwater pilae of the via Herculea.

239 3.2.2 Ground movements at Pozzuoli

240

241 While Via Herculea records the most ancient subsidence in the whole Campèi Flegrei area, the best
242 evidence for subsidence in the Pozzuoli area, where maximum ground movements have been
243 recorded, comes from Roman Market place, Serapeo, although subsidence in the Pozzuoli area is also
244 testified since Greek times (Gauthier, 1912).

245 Recent drilling has revealed four successively superimposed floors, ranging from the Augustan age
246 (31 BC-14 AD) to that of the Severi (193-235 AD), indicating a progressive subsidence (Fig. 5: from
247 Amato and Gialanella, 2013). Fig. 6 shows the time evolution of the approximate level of the
248 uppermost, 4th floor. It subsided below sea level in the 5th century (about 200 years after its
249 construction during the Severi Age). By the time it had reached 3.6 m bsl (around the 7th century
250 AD), the sediments had covered the base of columns (which formed the so-called "fill": Parascandola,
251 1947). Lithodomes colonized those parts of the columns near sea level (between 3.6 and 6.30 bsl: see
252 the two red arrows in Fig. 7c), creating pitted bands about 2.7 m thick above the sedimentary layers.
253 This process occurred until the 9th century AD, when the fourth floor was located to a depth of 6.3
254 m below sea level. In the same period, ground subsidence caused thermal and rain waters to flood the
255 Agnano plain, east of Pozzuoli, where they formed a new lake (Anzecchino, 1931). This indicates a
256 general persistence of subsidence in the Pozzuoli area (Fig. 7a; Appendix 2), contradicting the
257 conclusion by Morhange et al. (1999; 2006), that an uplift, of several meters, occurred in the period
258 7th-8th century.

259

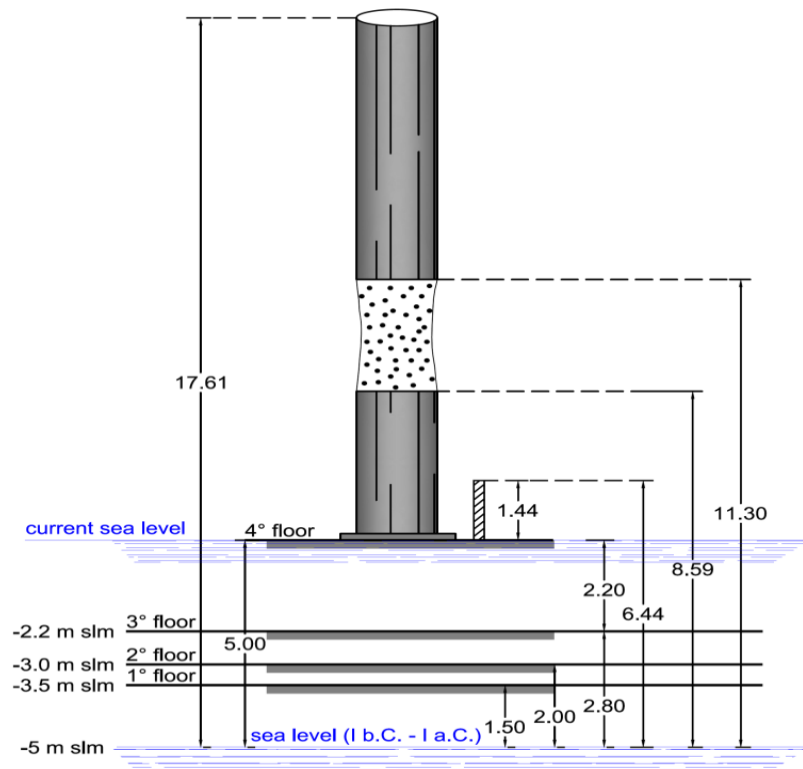


Fig. 5 – Floors underlying columns of Serapeo (redrawn from Amato and Gialanella, 2013). The dotted part of the column indicates the boring due to colonies of *Lithodomus Litophagus*.

Evidence for persistent subsidence comes from the Arab geographer Idrisi (11th century), from Benjamin ben Yonah de Tudela (12th century) and Nicolò Jamsilla (13th century), which describe the morphology of Rione Terra as a medieval castle surrounded by the sea on three sides (Costa et al., 2022: see points 6 and 7 in Appendix 2). Boccaccio (1355-1373) also reported that the fisherman's wharf in the Bay of Pozzuoli had become completely submerged (Parascandola, 1947: point 8 in Table 2 and Appendix 2).

As already discussed by Bellucci et al. (2006), we can obtain a more precise estimate of the depth below sea level reached by the Serapeo's 4th floor in the 15th century, by observing the painting "Bagno del Cantariello" (Fig. 7a), part of the famous Balneis Puteolanis of the Edinburgh Codex of 1430 AD (Di Bonito and Giamminelli, 1992). The painting depicts the Rione Terra encircled by vertical yellow tuff walls, from which the beach of Marina Della Postierla extends (towards the observer) to the base of the S. Francesco hill, the source of the thermal spring Cantariello (foreground) near the coast northeast of the submerged Serapeo. Behind the visitors of the thermal spring, the painting clearly shows the upper part of the three marble columns of the Serapeo above sea level. People are also shown fishing directly from the shore (Fig. 7b). From this painting we can make a rough estimate of the portion of columns below the sea level at that time, taking into account that a significant part of the columns is submerged. Historical records from the 1750 excavations, indicate

that the buried part of the columns amounted to about 10 m (see Parascandola, 1947). The uppermost 2 meters consisted of pyroclastic deposits of the 1538 eruption (see further paragraphs).

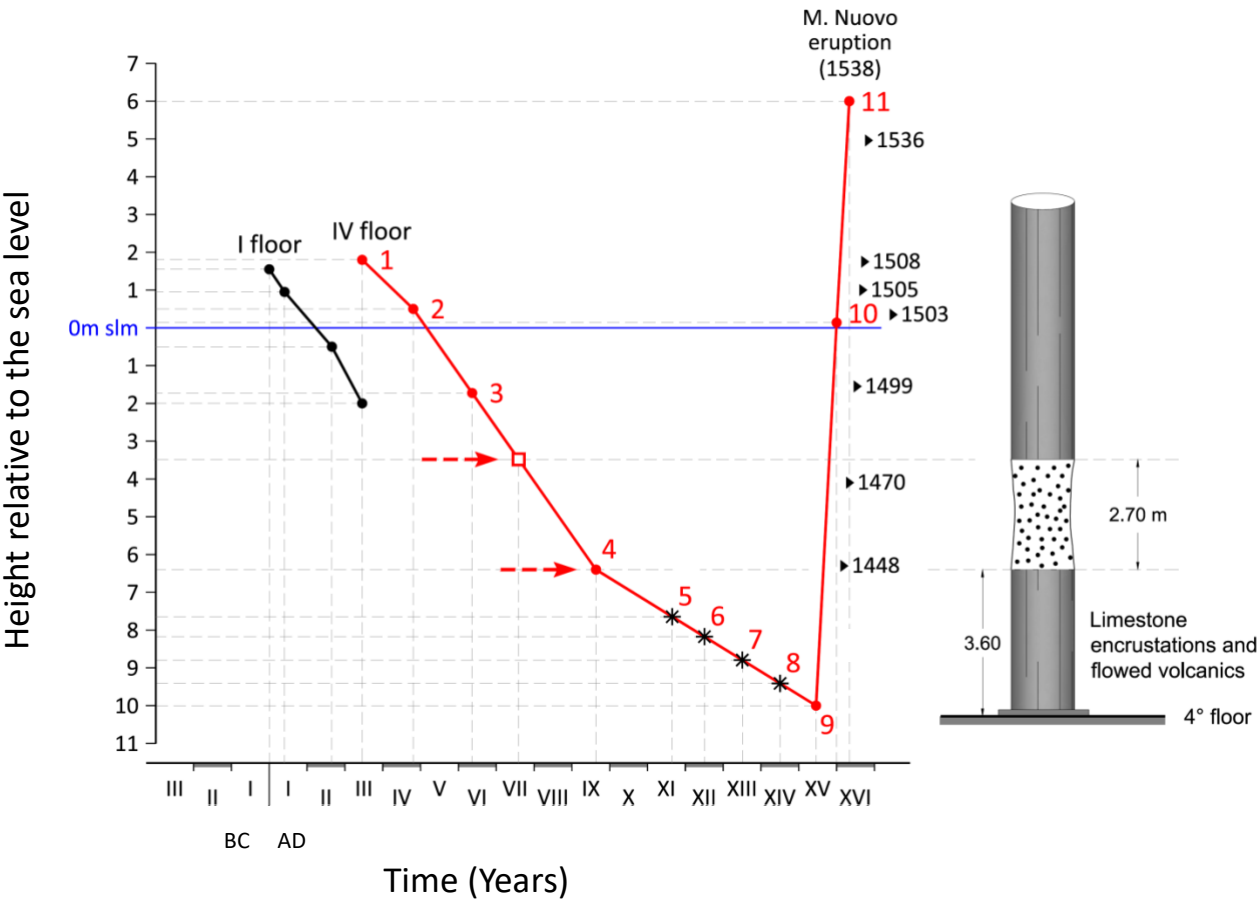


Fig. 6 – Diagram of the level of first (until the building of the fourth floor) and fourth floor of the Serapeum The arrows indicate the limits of the submersion corresponding to the part of the columns bored by lithodomes. Each point on the curve refers to a specific documented historical period, whose number indicates the reference for the inferred level. References are synthetically reported in Table 2 and extensively explained in the Appendix 2. Dates marked on the right indicate the times of occurrence of major earthquakes.

Number	Time	Event	Reference source
1	230 AD	The third floor of Serapeum was at a level of only about 1 m asl, often invaded by water: it was then built the fourth floor, located at 2 m asl	Amato and Gialanella, 2013
2	394 AD	The fourth floor is invaded by the sea. Important works to restore the banks and protect them by coastal embankments	Camodeca, 1987; Caruso, 2004

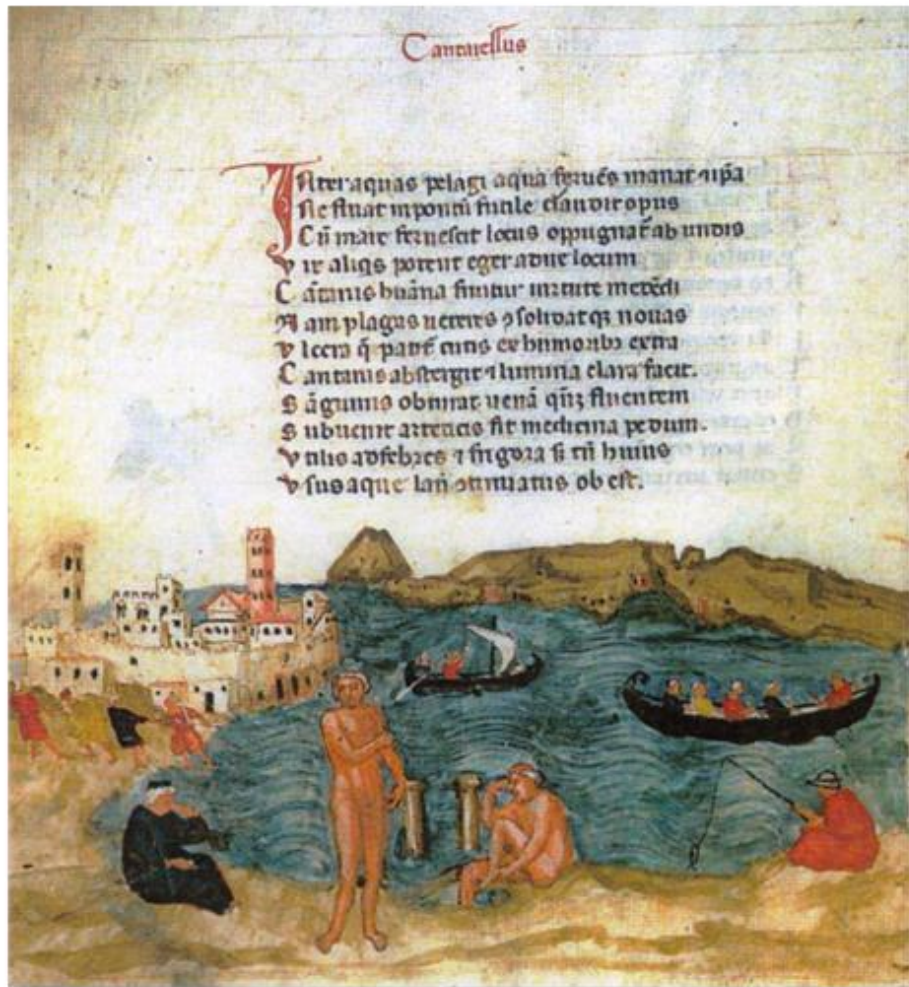
3	VI-VII century	Puteoli almost depopulated. People refuged in a fortified citadel, surrounded by sea: the Acropolis of Rione Terra	Varriale, 2004
4	VIII-X century	Due to continuous subsidence, Agnano Plain was invaded by water, transforming into a lake	Annechino, 1931
5	XI century	The sea increasingly surrounded Rione Terra, which appeared like a castle. The Arab geographer <i>Idrisi</i> in his <i>Opus Geographicum</i> , describing Pozzuoli as a "castle"	Varriale, 2004
6	XII century	Subsidence continues: Benjamin ben Yonah de Tudela, passing through Pozzuoli, described: <i>turres et fora in aqua demersa quae in media quondam fuerant</i>	Russo Mailer C., 1979; Caruso, 2004
7	XIII century	Subsidence continues: Niccolò Jamsilla (<i>Historia de rebus gestis Frederici II imperatoris ejusque filorum Corradet Manfredi Apuliae et Siciliae regnum</i>) describes the places between Agnano and Pozzuoli as follows: <i>...videlicet Putheolum mari mantibusque inaccessibilius circumquaque conclusum...</i>	Fuiano, 1951
8	1327-1341	Boccaccio reported descriptions as the lower part of Puteoli being completely submerged	Mancusi, 1987
9	1430	The 1430 gouache 'Bagno del Cantariello' shows the Serapeum columns submerged	Di Bonito and Giamminelli, 1992

		for about 10 meters. A	
10	1441	A description indicates that ‘the sea covered the littoral plain, today called Starza’	De Jorio, 1820

Table 2: Synthetic sketch of the main historical sources used to reconstruct the ground deformations shown in Fig.6 (see Historical Appendix 2 for more details).

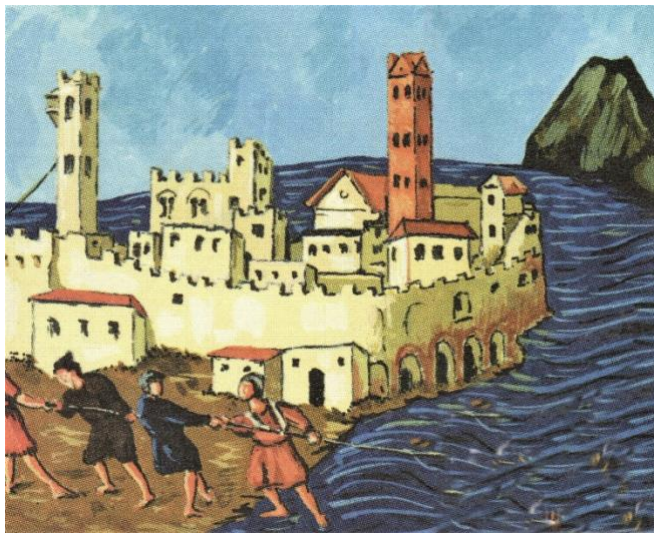
Before the eruption, therefore, the buried part of the columns must have been approximately 8 meters. The presence of trawling fishermen (Fig. 7b) suggests a depth of the sea of not more than 2 m (the maximum water depth for this type of fishing not far from the beach). Given that the total height of the columns is 12.7 m, we estimate that the emerged part of the column in 1430 was around 2.0-3.0 m (Fig. 7a,c), as already computed in Bellucci et al. (2006).

We therefore infer that in 1430 AD the floor was about 10 m (+/-1 m) below sea level (Fig. 6), and it is consistent with a topographic map of the Pozzuoli area in Roman times (Fig. 8a: Soricelli, 2007).

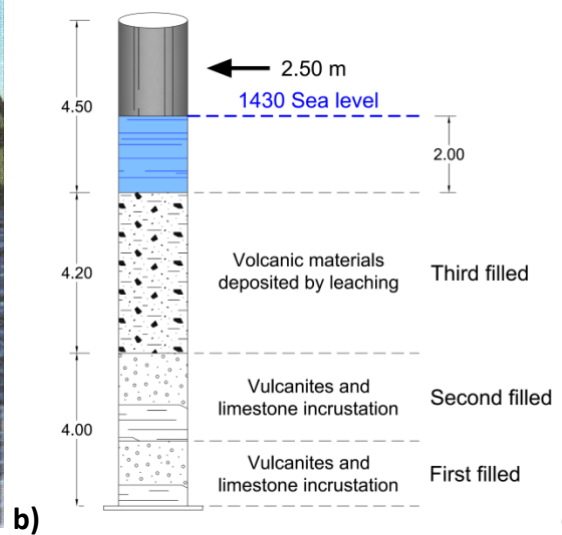


306

a)



307



b)

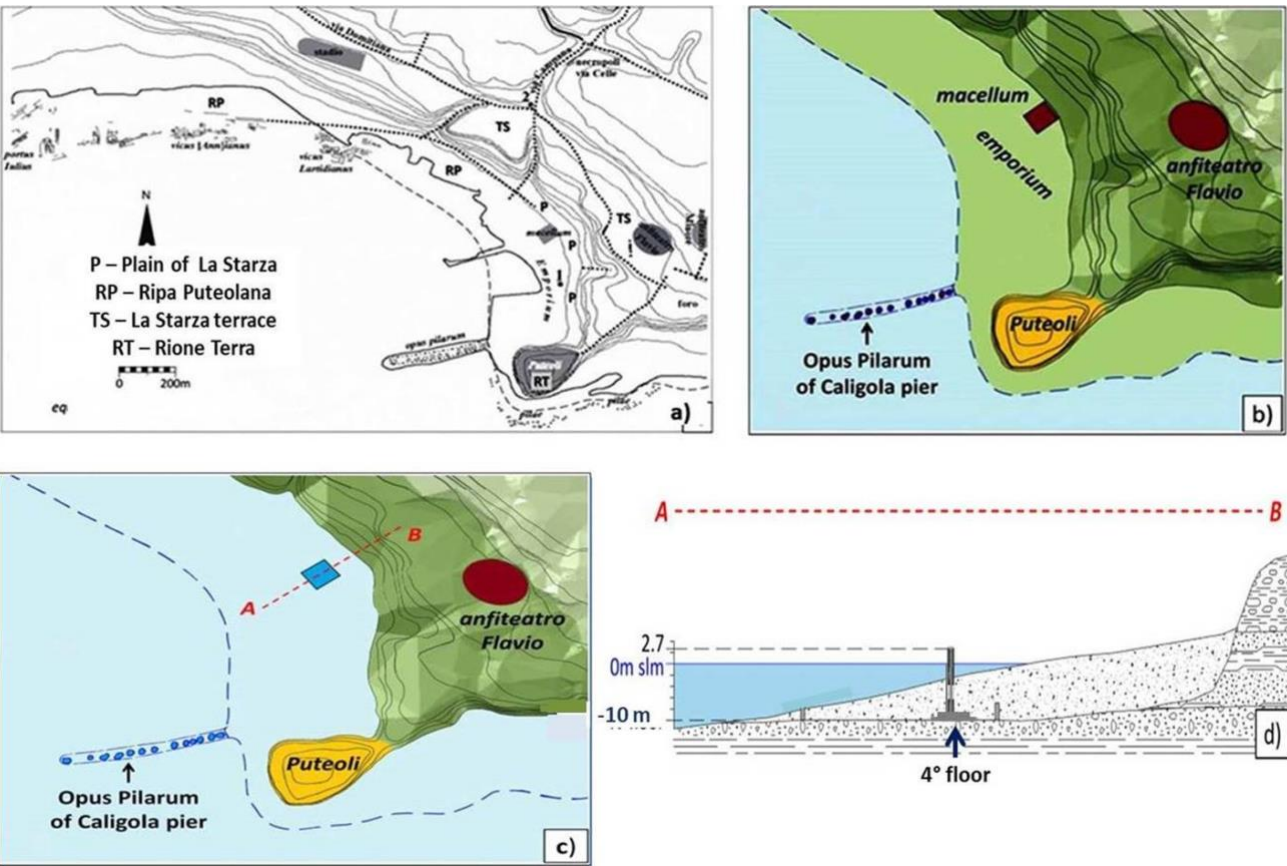
c)

308

309 Fig. 7 – Gouache of de' Balneis Puteolanum from 1430: a) Stumps of the Serapeum columns
310 that protrude from the sea to a height of 2-3m, b) Fishing from the shore, highlighted in the

311 box, indicates a draft depth of approximately 2m of sea, c) Reconstruction of the submerged,
 312 emerging and buried parts of the columns (see text for complete explanation).

313



314

315

316 **Fig. 8 – a) Map of Pozzuoli from the Roman era (III-IV century).** The map shows the lower part
 317 of the emporium which extends along the Puteolana bank (RP), until reaching the base of the
 318 hill, the so-called Starza plain (P) and the upper part of the Rione Terra cliff (RT) which, in
 319 turn, connects with the upper hilly part of the Starza terrace area (TS). **b) Part of the previous**
 320 **map, limited to the Emporium Area, in the Middle Age (after Aucelli et al., 2020, and Taravera,**
 321 **2021).** **c) the same area shown in b around 1430, during which the hill areas (TS, RT) were**
 322 **surrounded at the base by the sea, according to a description of the lower area of Pozzuoli from**
 323 **1441 "the sea covered the littoral plain, today called Starza" (after De Jorio, 1820; Dvorak and**
 324 **Mastrolorenzo, 1991).** **d) sketch of the profile A-B shown in c: the sea extended behind the**
 325 **Serapeum on the plain of La Starza hill, intersecting the columns at a height of 10m (also**
 326 **shown).**

327

328

329 The map (contour lines of 5m), shows that in the period of greatest development the city included the
330 Greek Acropolis (the ancient Dicearchia nowadays called Rione Terra), with a maximum height of
331 40 m asl, the lower part of the city, i.e. the western area overlooking the Serapeo, and the upper city
332 on the Starza terrace, with elevation between 30-50 m asl. The latter was the site of major public
333 works, such as an amphitheatre, stadium, forum and necropolis. From this map, a sketch of
334 topographical relief above the sea level (in Roman times, Fig. 8b) and underlying sea level (in 1430
335 AD, Fig. 8c) has been obtained as follows:

336 - from profile A-B (Fig. 8c,d) the 4th floor of the Serapeo can be located at 10m b.s.l., packed in the
337 sediments that form the Ripa Puteolana (RP), with the columns protruding from the same sediments
338 for 4.5m, of which approximately 2m are sea water. Sea level intersects the columns at a height of
339 approximately 10 m, connecting with the contour line of 10 m on the La Starza Plain (P) (Fig. 8c,d).
340 Fig. 8c also highlights the morphological conditions of the Rione Terra, which, as we have already
341 observed, has been described by the chroniclers who visited this place from the 11th to the 13th
342 century as "*an unapproachable mountain completely surrounded by the sea*" (Fuiano, 1951; Varriale,
343 2004, in Appendix 2).

344 The historical data presented here indicate several differences from previous reconstructions of
345 ground movements in the area very different from hypotheses appeared in previous literature. One of
346 the most recent works on such an argument (Di Vito et al 2016), for instance, made the following
347 claims:

- 348 1) the subsidence in the area started in 35 BC;
349 2) the local uplift in the area of the 1538 vent, from 1536 to 1538, amounted to about 19 m.;
350 3) the maximum subsidence was reached in 1251.

351 The first claim is in contrast with historical evidence that Via Herculea showed signs of subsidence
352 already at the times of Greek colonization (end of 8th century BC: see Diodoro Siculo in Appendix
353 1) (Fig. 2); in addition, Giulio Cesare himself was sent by the Roman Senate in 48 BC to fix the
354 problem, which was provisionally best resolved by Agrippa in 37 BC, raising the surface of the Via
355 Herculea with respect to the sea level (see again detailed explanation in Appendix 1).

356 The second claim is unrealistic, because an uplift in the Monte Nuovo area higher than few meters
357 would have raised the Via Herculea above the sea level (Fig.3d), which did not occur.

358 Finally, claim 3 is not confirmed by the testimonies collected until 1430, which instead indicate tha
359 subsidence continued beyond 1251, until 1430 at least (Di Bonito and Giamminelli, 1992; Bellucci
360 et al., 2006).

361

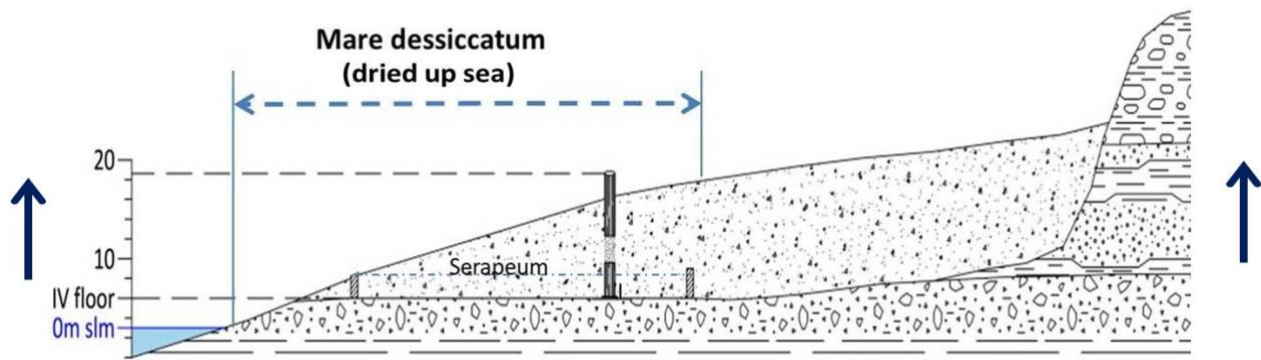


Fig. 9 – The uprise of the land (marked by the two arrows on the sides) was observed and described by Loffredo Ferrante in 1530: "the sea was very close to the plain which was at the foot of the Starza hill". In this context, the 4th floor of the Serapeum had reached a height of approximately 4 m above sea level.

Our findings date the starting phase of uplift to around 1430 consistent with the interpretations of Dvorak and Mastrolorenzo (1991) and Bellucci et al. (2006). They are supported by the documented occurrence of the first powerful earthquake documented in 1448 (Colletta, 1988: see also next paragraph), which induced King Ferdinand I of Aragon to suspend the so-called "fuocatico" (a mediaeval tax collected for each fire lit by a family unit; see Colletta, 1988). We know, from recent unrest, that earthquakes only occur during uplift at Campi Flegrei (Troise et al., 2019). It is also well known that, between 1503 and 1511, the municipality of Pozzuoli granted to citizens the new land that emerged as a result of the increasingly "drying up sea" (Fig. 9) (Parascandola, 1947).

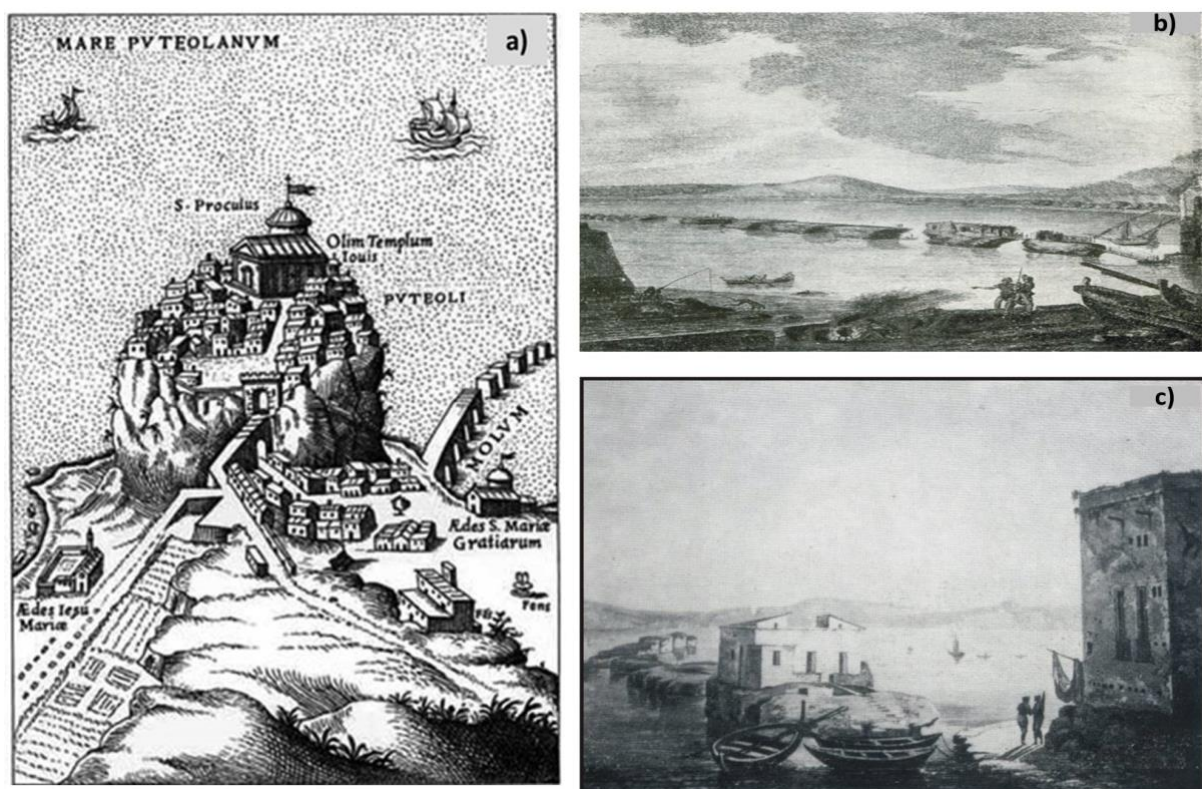
The next important question is then: was the 4th floor of the Serapeum above sea level as early as at the beginning of 16th century? Parascandola (1947) answered this question through a sentence found in an account by Loffredo Ferrante from 1580: *In 1503 the sea was very close to the plain which was at the foot of the Starza hill* (Fig. 8). So, it can be deduced that the floor of the Serapeo was just above sea level in 1503, that is it had risen about 10m in about 73 years, with a rate of 136 mm/y. There is clear evidence that the uplift phase continued until 1538, when the eruption occurred. The maximum uplift occurred in the Pozzuoli area, close to the Rione Terra cliff, and had reached up to 5-6 m asl by 1538 (Fig. 6).

At Averno, to the west, uplift was unable to raise Via Herculea above sea level. At Nisida island, to the east of Pozzuoli, the pier did not emerge above sea level (Parascandola 1947). Hence it is likely that the uplift phase had a bell-shaped trend, very similar to what we have seen in the recent unrests. Local large uplift occurred at the future site of Monte Nuovo just before eruption (around 48 hours before), indicating the rising of dyke, feeding the eruption. However, the total uplift there could have not been larger than about 7 m (the approximate depth bsl of the Via Herculea at the time).

390

391 4. Ground movements after the 1538 eruption

392 The period between the end of the 16th century and the beginning of the 17th century lacks written
 393 documentation about ground movements at Pozzuoli. It is likely that subsidence started after the
 394 eruption. Contemporary paintings provide constraints on when subsidence begin. The earliest, by
 395 Cartaro in 1584 (Fig. 10a), shows the Rione Terra in the foreground, with the Neronian pier almost
 396 completely above sea level, which means for about 5-6 m.



397

398 **Fig. 10 – a) Engraving by Cartaro (1584) showing the Neronian pier at the base of the Rione**
 399 **Terra, emerging from the sea for 5-6m, showing 10 of the 15 piles of which it was made up in**
 400 **roman epoch; b) The remains of the pier piles, without the upper arches, highlighted in an**
 401 **engraving of 1750; c) Detail of the same piles highlighted in another engraving from the same**
 402 **period (mid-18th century), where the height of the 1-2m piles is observed in more detail, subject**
 403 **to marked erosion**

404

405 The pier also appears still partially complete, with about half pylons still connected with arches (*Opus*
 406 *Pilarum*). In comparison, paintings from the middle XVIII century (Fig. 10b,c) show the pier
 407 completely destroyed and almost submerged. The painting in Fig. 10c shows the pylons in more detail,
 408 allowing their height to be estimated at 1-2 m asl.. Fig. 11, from Hamilton (1776), shows similar ruins
 409 for the Neronian pier: Hence it appears that the pier subsided of 5-6 from 1580 to 1776. Fig. 11 also
 410 indicates that the floor of the Serapeo was almost at the same level than the pier in 1776.

411



412

413 **Fig. 11 – a) View of the Gulf of Pozzuoli and the Cape Miseno peninsula (Hamilton 1776).**

414 **Both the remains of the Neronian pier and the newly excavated Serapeo are also visible**

415



416

417 **Fig. 12 – Illustration of Serapeum, as excavated in the three-year period 1750-1753. It can be**
418 **noted that the height of the lighter parts of the columns, including the pitted band of the**
419 **lithodomes, is preserved by oxidation, because packed by the just removed sediments. The**
420 **darker upper part, oxidized since staying outside the cover, has a height of approximately**
421 **2.50m, estimated on the same figure. This leads us to consider that the pack of sediments**

422 removed had a thickness of approximately 10m, that is, the height of the hill where the *vineyard*
423 *of the three columns* was located before the excavation (Niccolini, 1842).

424

425 Its level in 1538 can therefore be estimated at 5 – 6 m. above sea level (Fig. 6), and about 1m above
426 sea level in 1750, with an estimated subsidence in 1580-1750 of about 4-5 m. This estimate is
427 consistent with measurements by Niccolini (1846, reported by Parascandola, 1947), who found the 4th
428 floor of Serapeo to have a height above sea level varying in the range 0.9 - 0.6m throughout the 18th
429 century. During the excavations of 1750 (Fig. 12) the floor could have hence been approximately at
430 0.7 m above sea level.

431 Since the Serapeo floor is at the same level of the Neronian pier (Fig. 11), elevated 5-6 m above the
432 sea level in 1584 (Fig.10a), recalling it was 10 m below sea level in 1430 and the total uplift was 16
433 m, we deduce that significant subsidence did not start before 1580-1584. Parascandola (1947),
434 hypothesized that the subsidence of 4 - 5 m, started after 1580, could have evolved at higher initial
435 rate, in such a way that, around the middle of the 17th century, it already had a value of 2 -3 m, and
436 then slowed down towards the end of the century, until the 1750. This likely hypothesis has been
437 taken into account in the reconstruction of Fig.13.

438 It is also interesting to compare the average subsidence rate before 1430 with that observed between
439 1538 and 1950. The overall rate of subsidence after 1538 is more than 2 cm/year, almost double with
440 respect to that observed before 1430. Actually, also excluding a likely first phase of sharp subsidence
441 occurred just after the 1580, the subsidence rate observed before 1950 remains significantly higher
442 than that observed since the roman era until 1430.

443 Since the 1850s, survey data have recorded ground movements at Campi Flegrei with increasing
444 precision. The Military Geographic Institute (IGM), in particular, started frequent high precision
445 levelling surveys in 1950. Data from the levelling surveys were still provided also during the
446 occurrence of the most recent unrest phases, i.e. in 1950 - 52, 1969 – 72, 1982 – 84 and until 2001.
447 Since 2001, continuous measurements have been provided by GPS stations, including station RITE
448 installed at Rione Terra (Del Gaudio et al 2010; see Fig.13).

449

450

451

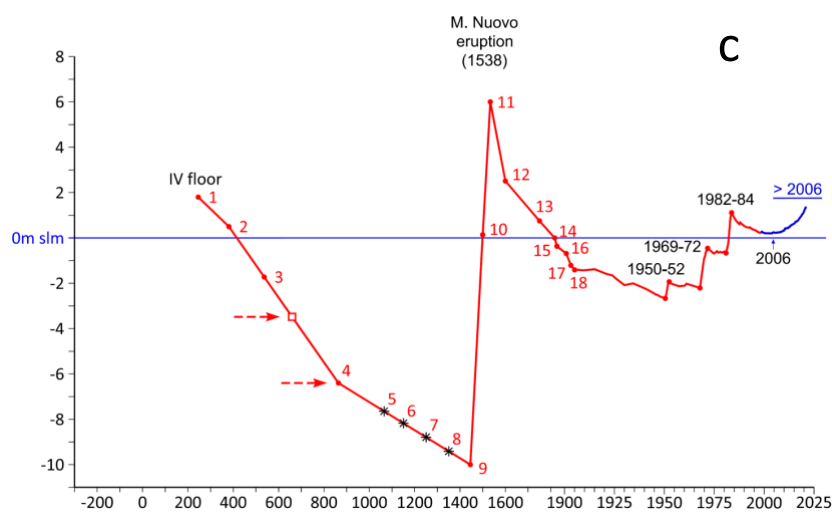
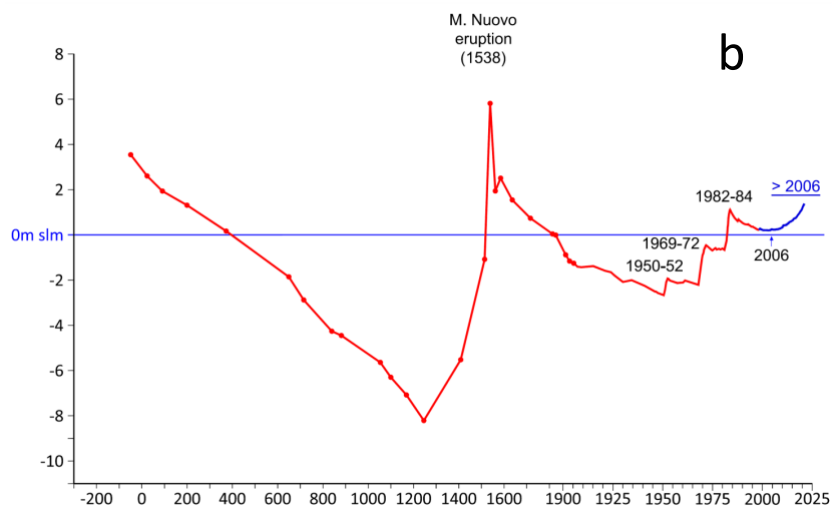
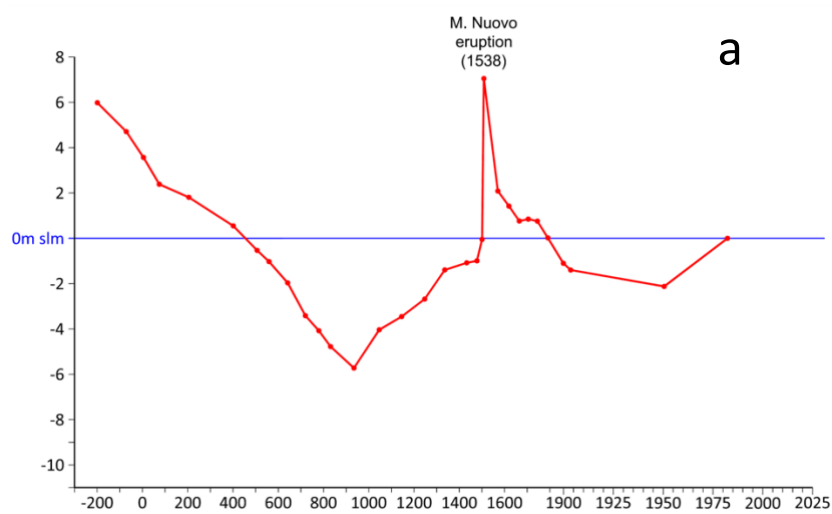
452

453

454

455

Height relative to the sea level



Time (Years AC)

490
491
492
493
494
495
496
497
498
499
500
501
502
503
504
505
506
507
508
509
510
511
512
513
514
515
516
517
518
519
520
521
522

Fig. 13 a) Reconstruction of the ground level of the Serapeum floor, with respect to the mean sea level (blue line), as proposed by Parascandola (1947); b) Reconstruction of the Serapeum floor ground level, recently proposed by Di Vito et al. (2016); c) Reconstruction of the ground level of the Serapeum IV floor, since III century A.D. to present, inferred by this study. Each point in the diagram corresponds to an appropriate historical indication reported in Table 1 and in the Appendix 2.

5. Schematic model for the preparatory phases of the 1538 eruption

5.1 Dynamics of the resurgent block in response to temperature and pressure perturbations

Ground deformation at Campi Flegrei, before and after the 1538 eruption, appears to have been concentrated in a small area, a few km in radius, around Pozzuoli, similar to that observed during unrest since 1970 (De Natale et al., 2001; 2006; 2019). Such a concentration agrees with the presence of a resurgent block.

Evidence for resurgent block movement during unrest was first highlighted by De Natale and Pingue (1993), who pointed out that the concentration of the uplift in a small area, the high uplift values, and the invariance of the uplift and subsidence shape, as well as of the seismic area, was consistent with the up and down movement of a block bordered by ring faults (see also De Natale et al., 1997; Beauducel et al., 2004; Troise et al., 2003; Folch and Gottsmann, 2006). A resurgent block, mostly detached from the external caldera rocks, would also favour the almost constant, highly concentrated shape of ground displacement, during both uplift and subsidence. Active high-resolution reflection seismic surveys have imaged the presence, in the Gulf of Pozzuoli, of an inner resurgent antiformal structure or “block” bounded by a 1-2 km wide inward-dipping ring fault system associated with the caldera border, whose limits have been also documented by the survey (Sacchi et al., 2014 Steinmann et al, 2016; Sacchi et al., 2020a). Further constraints for the extent on-land of the resurgent block come from stratigraphic evidence. In particular, the old well CF-23, drilled in the Agnano area, presents about 900 m of NYT deposits, topped by only 100 m of more recent deposits (Rolandi et al. 2020b). The presence of uplifted, thick layers of NYT, characterizes the stratigraphy of all the wells contained in the resurgent block (Fig.14a,b,e), thus allowing to map its extent on-land, although only the CF-23, by far the deepest one, clarifies the whole thickness of the NYT deposits in the resurgent area (Fig. 14a,c,d).

523 The extent of the resurgent block on-land appears also reasonably well defined by a clear relative
524 gravimetric maximum (Capuano et al., 2013). The resurgent structure is also associated with distinct
525 seismicity along the bordering ring fault zone (see also Troise et al., 2003). Fig. 15a-c shows how the
526 resurgent block is well shown by passive seismic data (Fig. 15b, c) and by earthquake locations (Fig.
527 15a; see Troise et al., 2003).

528 The presence of the central, resurgent block significantly affects the dynamical behavior in response
529 to temperature and pressure perturbations. This is particularly evident in the central, most deformed
530 and seismic area, where the shallow crust involves approximately 1.5 km of lithoid tuff. This
531 contradicts substructure models proposed by various authors (Rosi and Sbrana, 1987; Vanorio et al.,
532 2002; Lima et al., 2021; Kilburn et al., 2023), which often assume a thick shallow layer of loose
533 pyroclastics from recent eruptions, typically represented by the stratigraphy of well SV1 (see Fig.
534 14e). We stress that deposits from recent eruptions are not lithoid in character because almost all of
535 them, except very few, did not experience zeolithization, which only occurs with high temperature
536 and high water content (REFERENCE?).

537 The physical state of the shallow structure within the resurgent block can be inferred by seismic
538 tomography analyses presented by several authors (e.g. Aster and Mayer, 1998; Vanorio et al., 2005;
539 Vinciguerra et al., 2006; Battaglia et al., 2008; Calò and Tramelli, 2018). These analyses consistently
540 indicate a high V_p/V_s ratio centered below Pozzuoli town down to 1-2 km, interpreted as highly water
541 saturated tuff.

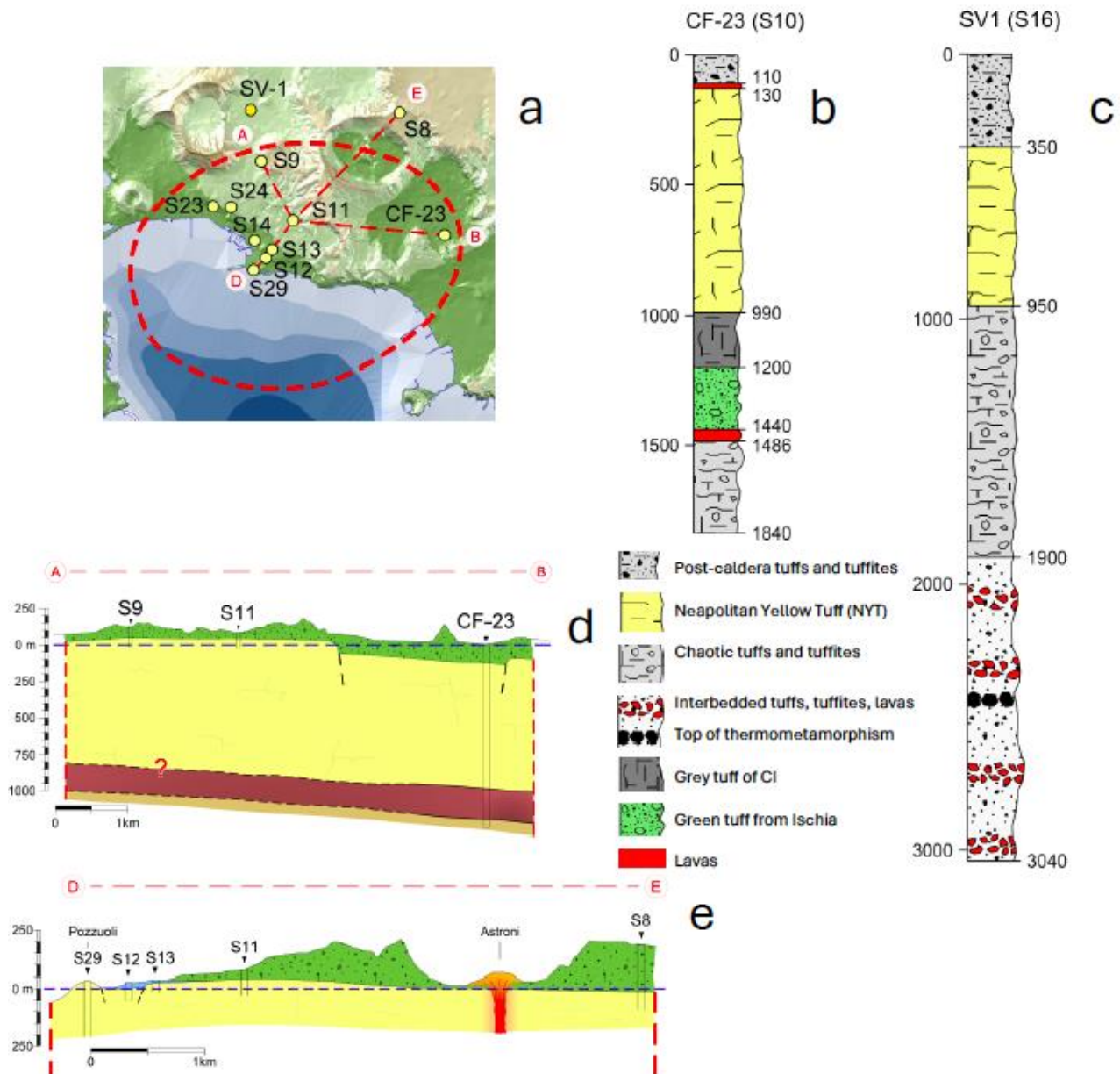
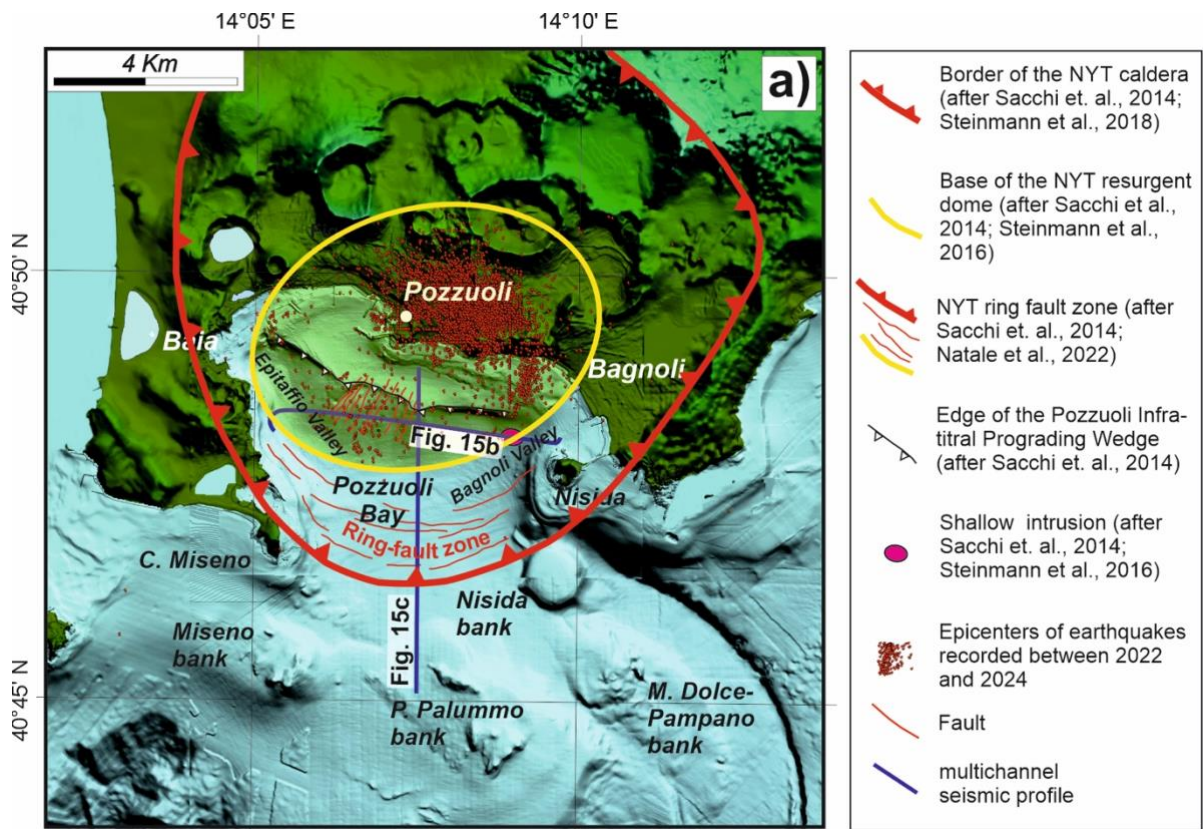


Fig. 14 - a) Location of the wells explored within the resurgent tuff block, as reported in literature; b) Stratigraphy of the CF23 (S10) well, within the resurgent block; c) Stratigraphy of the SV-1 well, outside the resurgent block, which highlights a stratigraphy where the NYT tuff blocks are not present with significant thicknesses; d-e) Profiles in the resurgent block which highlight the shallow depth of NYT because of the resurgence.

Of particular significance is the work by Vinciguerra et al. (2006) which compared the results of seismic tomography with laboratory tests. They demonstrated that the tuffs present in the central area of the Campi Flegrei caldera can be either water or gas saturated, and that inelastic pore collapse and cracking produced by mechanical and thermal stress can significantly alter the velocity properties of Campi Flegrei tuffs at depth. The effect on velocities becomes significant when the temperature rises

554 sufficiently to induce physical changes, such as volume change and the generation of free water
 555 associated with the dehydration of zeolite phases. This can lead to thermal crack damage (see also
 556 Chiodini et al., 2015; Moretti et al., 2018), further affecting the dynamic behavior of the area. At
 557 higher depths, the well CF-23 indicates the presence of pyroclastic deposits from a depth of
 558 approximately 1.5 km to at least 1.8 km, where a temperature of 300°C was measured (Fig. 14b).
 559 Likely, at even greater depths of about 3km, marine silt and clay layers induce silica mineralization
 560 and the formation of low-permeability horizons. Due to the high temperatures, estimated to be at least
 561 400°C, these layers undergo thermal alteration, forming a thermo-metamorphosed layer (Fournier,
 562 1999; Lima et al., 2021; Cannatelli et al., 2020).
 563 In addition, Battaglia et al. (2008) interpreted a low Vp/Vs body, a imaged to a depth of about 3–4
 564 km, as due to the presence of fractured, overpressured gas-bearing formations, confirming the data of
 565 Vanorio et al. (2005). This depth range of 3-4 km likely represents a primary accumulation zone for
 566 shallow intruded magma,
 567

568



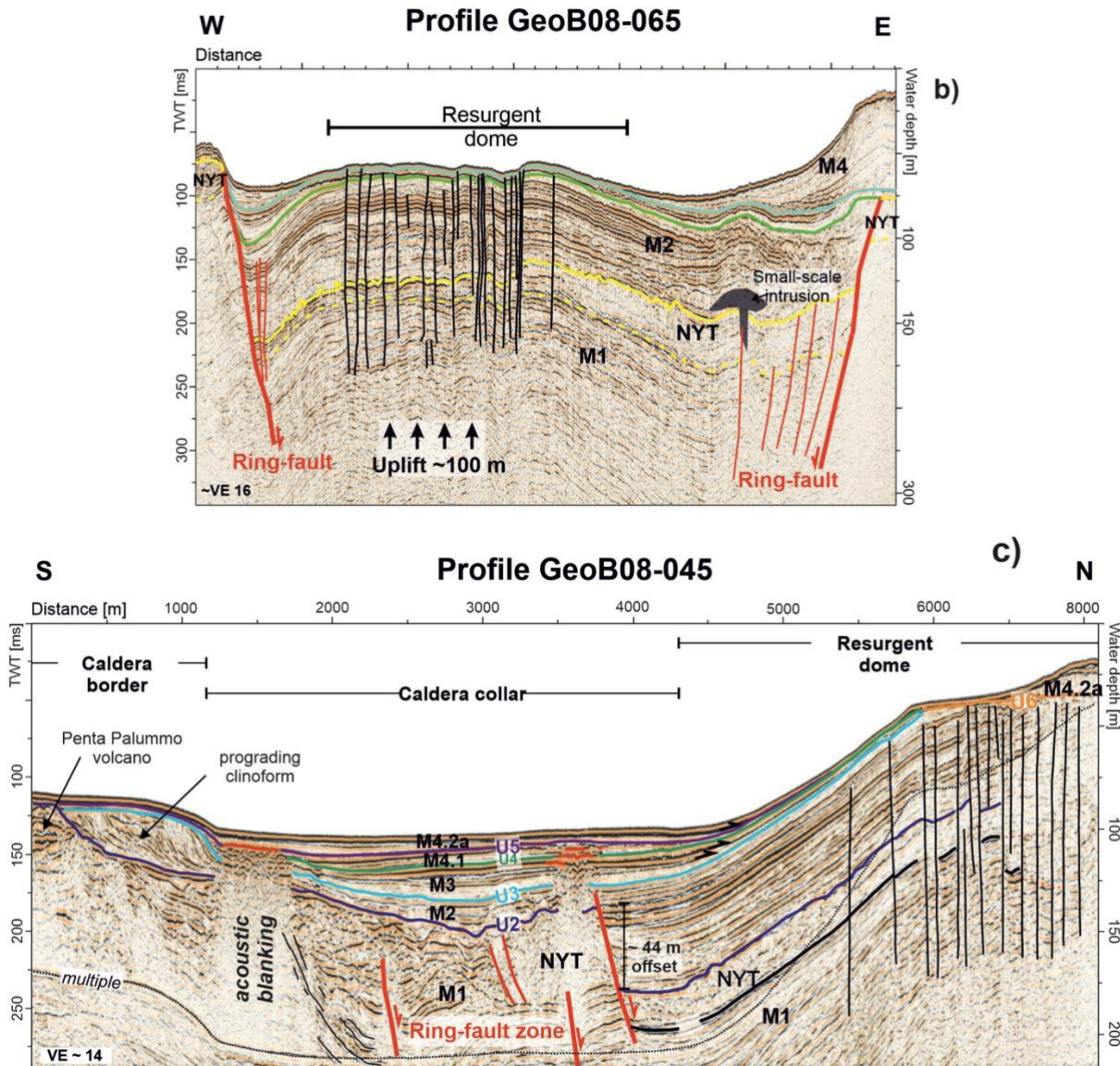


Fig. 15 – a) Campi Flegrei map showing the approximate limits of the resurgent block (area in the yellow ellipse), which concentrates ground deformation and seismicity. b) The N-S and c) W-E profiles of the high-resolution seismic survey, showing the offshore signature of the NYT ring fault system and resurgent structure (from Sacchi et al., 2014, 2020a, 2020b; Steinmann et al., 2016).

which is unable to reach the surface and instead forms magma sills (Woo and Kilburn, 2010; Di Vito et al., 2016; Troise et al., 2019; Kilburn et al., 2023). The magma at this depth could be in a mush state, i.e. solidified but still at temperature high enough to be remobilized by the inflow of new magma or hot magmatic fluids (De Natale et al., 2004).

At even greater depths, approximately between 7 - 8 km, the main magma chamber is located. This chamber contains both liquid magma and residual mush from past eruptions (Zollo et al., 2008).

5.2 The preparatory phases of the 1538 eruption

A tentative model can be now constructed for the preparatory phases of the 1538 eruption, which accounts for all available data. It is shown in Fig. 16, and can be summarized as follows: the Pozzuoli area experienced a long period of subsidence, beginning at the end of the second phase of post-caldera volcanism (3.7 ka B.P.) and lasting until 1430 AD. This subsidence was likely triggered by the collapse of the upper and middle crustal blocks into the underlying magma chamber, situated deep within the limestone basement at depths of 7-8 km (Zollo et al., 2008). Any viscoelastic behaviour of the shell encasing the magma chamber may have also contributed to the subsidence, along with the decrease in magma volume due to cooling and crystallization (Fig. 16a).

Since the end of the second phase of post-caldera volcanism, approximately 3.7 ky ago, the primary magma chamber, located at 7-8 km of depth, likely contains a mixture of liquid magma and mush. It's important to note that mush refers to a non-eruptible phase of trachytic magma, composed of 25%–55% volume by crystals (Marsh, 1996; Bachmann and Huber, 2016; Cashman et al., 2017; Edmonds et al., 2019). When heated by several tens of degrees, typically through the injection of hotter magma, mush can revert to a liquid state, thereby regaining the ability to trigger a volcanic eruption (e.g. De Natale et al., 2004; Caricchi et al., 2014). However, the way the mush is rejuvenated by intrusion plays a fundamental role in this mechanism (Parmigiani et al., 2014). One plausible scenario is that the new magma from the deeper crustal levels forms sills at the base of the mush, revitalizing it through the supply of heat, but not of magmatic mass, i.e. only exsolution occurs (Bachmann and Bergantz, 2006; Bergantz, 1989; Burgisser and Bergantz, 2011; Huber et al., 2011; Bachmann and Huber, 2016; Cashman et al., 2017; Carrara et al., 2020). The rapid uplift observed in the interval between 1430 and 1538, could be explained by the temperature contrast between the two layers: the mafic melt positioned at the base, being hotter than the overlaying layer, undergoes cooling and crystallization, leading to an increase in the volatile content (primarily H₂O and CO₂) of the residual melt (Fig. 16b). Lower ductile rocks tend to deform gradually, allowing magmatic gases to permeate into the brittle zone above, thereby inducing a thermo-metamorphic separation layer.

A seismic anomaly displaying low V_p/V_s at about 3-4 km depth (Battaglia et al., 2008) indicates the presence of supercritical fluids. Earthquakes are clustered above such a depth, because rock rheology is ductile at supercritical temperature, also suggesting the presence of both fractured rocks and overpressured gas. This condition likely results in triggering additional earthquakes (Fig. 16a): a similar condition has been often hypothesized to occur in the Yellowstone volcano (Shelly and Hurwitz, 2022), and is explained in the following. Intense degassing from the main magma chamber would lead to increased pressure in the shallow aquifers forming the large hydrothermal system, just as hypothesized for recent unrest (Moretti et al., 2017; 2018); moreover, the rise in temperature would

617 cause the water contained in the tuffs' zeolites to convert into steam, generating additional
618 overpressure. Such a situation is shown by the CF-23 well, where its stratigraphy indicates the
619 presence of a magmatic layer approximately 30 m thick beneath the overlying tuff blocks, which are
620 approximately 1.5 km thick (Fig. 14b).

621 It is noteworthy, when considering the correct stratigraphy of the resurgent block as represented by
622 the CF-23 well, that some previous models suggesting the presence of two low-permeability layers
623 at depth (Vanorio and Kanitpanyacharoen, 2015; Kilburn et al., 2023), inferred from the SV1 well
624 (which is situated outside of the resurgent block) (Fig. 14a), can be questioned.

625 Finally, super-compressed magmatic gases were likely contained within an approximately 2.5 km
626 thick fragile zone (from about 1.5-2.0 to 4 km of depth), while a limited release of the increased
627 pressure occurred directly through the fractures connecting the intermediate depth area with the
628 Solfatara and Pisciarelli areas, resulting in the escape of CO₂-rich vapour. A similar mechanism has
629 been evidenced in the recent unrest, by the reported increase in fumarolic activity and in the CO₂/H₂O
630 ratio (Chiodini et al. 2021).

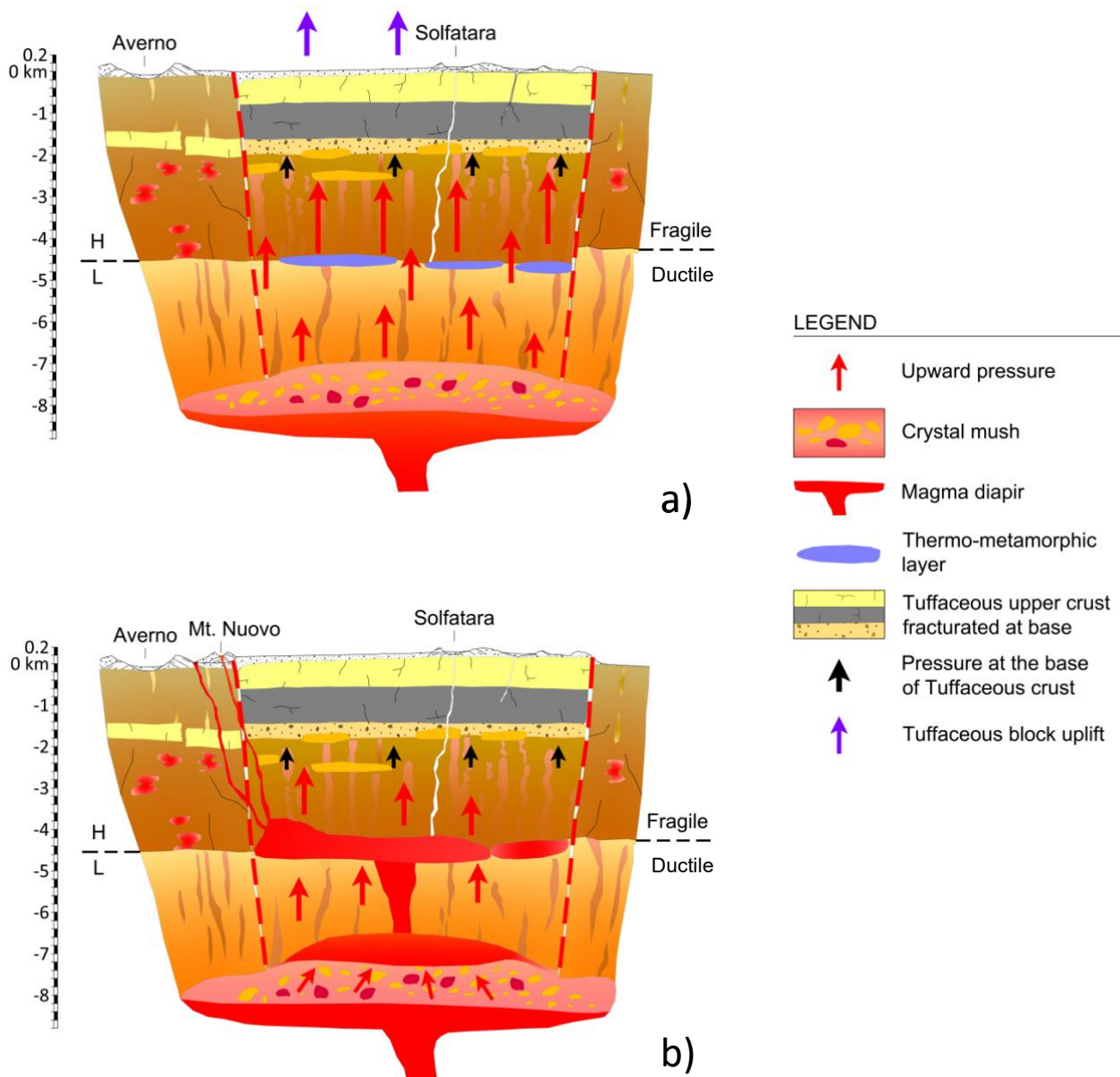
631 Following this hypothesis, it is noteworthy that, at a depth of 1.8 km, the CF23 drill-hole indicates a
632 very high temperature of 300°C, not far from the supercritical temperature. It is plausible that, if the
633 temperature significantly increases, due to the supply of deeper, hot magmatic fluids, the water
634 contained in the basal part of the tuff block could reach supercritical conditions, leading to thermal
635 fracturing within the tuff block (Vinciguerra et al., 2006), over a certain thickness (Fig. 16b).

636 As previously mentioned, the increase of pressure resulting from such intense heating caused by deeper
637 magmatic fluids should be attributed to both the overpressure of shallow aquifers and the vaporization
638 of water contained in the zeolites, likely in the form of superheated steam.

639

640 The pressure increase in the main magma chamber, resulting from the input of new magma and/or
641 magmatic fluids as explained, can also trigger the formation of magma dykes (Troise et al., 2019).
642 The progressive intrusion of several magma dykes likely leads to the ascent of magma towards the
643 surface. This process may be further facilitated by phreatic explosions caused by the heating of
644 shallow aquifers, resulting in depressurization pulses. Intruding magma may encounter layers that are
645 more resistant to penetration at certain depths. In this case further magma intrusion may be inhibited
646 and lateral expansion, to form sills, may occur (Gretener, 1969). Previous studies of recent unrests
647 have indicated that depths between 2.5 and 4 km, close to the upper limit of the ductile zone, are
648 locations where magma intrusions can halt (Woo and Kilburn, 2010; Troise et al., 2019). Before the
649 1538 eruption, a small plumbing system, in the form of flattened intrusions near the contact between
650 a lower ductile zone and an upper brittle zone in a high-pressure environment, was hypothesized (Fig.

651 16b) (Pasquarè et al., 1988). From such a shallower magma chamber, magma can further progress
652 upward towards the surface. A dynamic in which early intrusions in the shallow crust create small
653 plumbing systems (i.e. stalled intrusions), from which a dyke later propagates, bringing a small
654 quantity of magma to the surface, is typical of monogenic volcanoes (Marti et al., 2016). The ability
655 of intruded magma sills to erupt at surface is also influenced by the relatively short timescale of sill
656 solidification, typically in the order of few tens of years (Troise et al., 2019).
657 Shallow magma sills, in the form of mush, can be remobilized due to the arrival of new magma and/or
658 of hot deeper magma fluids. The significant uplift preceding the 1538 eruption, amounting to more
659 than 16 meters in the initial phase involving the entire resurgent block, if interpreted solely in terms
660 of magma intrusion, would suggest a total intruded volume, in the shallow plumbing system, on the
661 order of some cubic kilometers of magma (Bellucci et al., 2006).



681 **Fig. 16 – Schematic cross sections of the hydrothermal and magmatic systems underlying the**
 682 **Campi Flegrei resurgent block in the 1538 AD, showing:**

683 **a) Process of gas sparging according to Bachmann and Bergantz (2006) model, related to the**
 684 **transfer of hot gas from a mafic intrusion underplating the trachytic mush and the hypothesized**
 685 **relation with earthquake swarms of the exsolved fluids, accumulated at lithostatic pressures in**
 686 **the ductile region and episodically injected into the brittle crust at very high strain rates. The**
 687 **sudden increase of fluid pressure, in the brittle region, can trigger earthquake swarms in the 2-**
 688 **4 km depth range.**

689 **b) Remobilization of mush by mafic magmas then occurs, so the magma remobilized from the**
 690 **mush accumulates at the top, fueling its rise upward to accumulate, in a sill-like shape, along**
 691 **the ductile-brittle transition surface. Eruption from the magma sill is then likely to occur at the**
 692 **faulted borders of the resurgent block.**

693

694 However, despite such a large uplift, suggesting however high volumes of shallow intruded magma,
695 the eruption of 1538 only produced about 0.03 km³ of pyroclastic deposits (see next section). This
696 discrepancy likely suggests that multiple sill intrusions occurred over more than one century, with
697 most of them solidifying without contributing to the eventual eruption. Only the most recent intrusion
698 events, and/or some portion of magma mush from prior intrusions remobilized by subsequent heating,
699 would have fed the eruption.

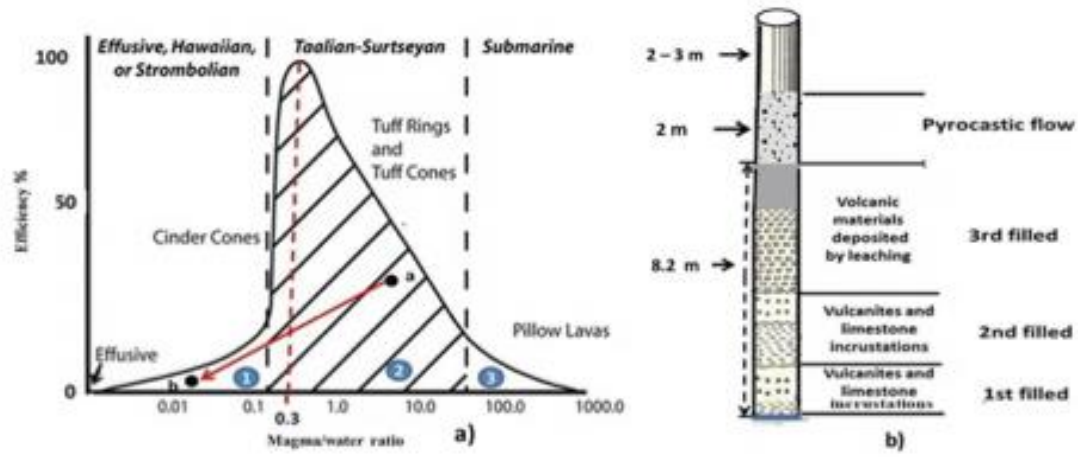
700 Also interesting is to note that, after the 1538 eruption, ground subsidence recovered only 8 meters,
701 i.e. one half of the former total ground uplift. This means that about one half of the total uplift may
702 have been caused by thermally pressurized gas and water (shallow aquifers), perturbed by hot fluids
703 coming from the deeper (7-8 km) magma chamber; the remaining, unrecovered uplift, should have
704 been caused by shallow magma intrusion. It is the same process hypothesized for recent unrests: in
705 particular, the 1982-1984 uplift showed a subsequent subsidence about one half than the former uplift,
706 interpreted as the deflation of formerly pressurized water and gas (Troise et al., 2019).

707 Another characteristic of eruptions from small monogenic volcanoes is their difficulty to be
708 forecasted, as they occur at unexpected locations (Marti et al., 2016). Both distinctive traits were
709 evident in the eruption of Monte Nuovo, which represents a prototype of a small monogenic volcano
710 in the Campi Flegrei. Despite the relatively small volume of magma (0.03 km³), the eruption occurred
711 at a considerable distance, approximately three km westward, from the area of maximum uplift. The
712 position of the 1538 vent is approximately on the border of the resurgent block: such a border, marked
713 by ring faults, clearly represents a weak zone, where magma can more easily intrude.

714 **5.3 The eruption of 1538**

715 The week preceding the eruption was marked by a series of seismic events (Guidoboni and Ciuccarelli,
716 2011). The shoreline gradually retreated 200 steps (ca. 370m) seaward, because of an occasional uplift
717 occurred on the eastern shore of Lake Averno (see Fig. 2d) and during the 36 hours preceding the
718 eruption, the ground level reached 7 meters of total uplift (Parascandola, 1943; Costa et al., 2022). The
719 local uplift rapidly attenuated as a function of distance (Rolandi et al., 1985) (Fig. 6). The uplift,
720 involving a local marine regression, was accompanied by strong rumbles on the night between 28 and
721 29 September, culminated in a further explosion, at 2 am on the following night, which marked the
722 vent opening and the start of the eruption. The early eruptive column, initially white in colour, ejected
723 muddy ashes and lithic and scoriaceous lapilli upwards. The presence of wet ash on the slopes of the
724 gradually growing volcanic cone led Parascandola (1943) to hypothesize that it was a mud eruption.
725 This description, present in the chronicles of the time (Parascandola 1943), indicates that the first
726 eruptive phase was phreatomagmatic in character, although it evolved with a peculiar characteristic,

752 2) If the water content increases, the efficiency drops because not all water is vaporized, and, as a result
753 steam saturated with water is formed. Under this condition, Pyroclastic flows are formed.
754 This last type of flow is therefore associated with the collapsing eruptive column that developed in the
755 night between 29 and 30 September, to be ascribed to a phreatomagmatic eruption with a high magma-
756 water ratio, which gave rise to the non-welded ignimbrites described in typology 2 and located in the
757 diagram of Fig.18a, at point a. Such particular condition for the flow, besides forming the new cone,
758 also formed pyroclastic flows directed towards Pozzuoli. This kind of flow deposit, 5 m thick, is
759 recognized in the tunnel of the new road to Arco Felice, located about 1 km from the cone (Fig.18c).
760 These deposits, never described before, also easily explain the two meters of M. Nuovo eruption
761 deposits described at Serapis Temple of Pozzuoli during the excavations (Parascandola, 1947), and
762 formerly ascribed to fall products (fig.18b). This implied that in the initial phase of the eruption the
763 magma absorbed a considerable quantity of sea water present above the eruptive vent, so in these
764 conditions, the collapsing eruptive columns which gave rise to the pyroclastic flows on the night
765 between the 29th and 30th September, reached a maximum height of less than 3 km, (Parascandola,
766 1943), depositing in a radius of approximately 3 km, as follows:
767 - with thickness of 5-10m, in sections obtained by cutting the slope in the area around the volcano (Fig.
768 17a);
769 - in a depression on the SE sector of the volcano. The materials of the Tuff Cone of Monte Nuovo (T)
770 are present, together with the products of the scoria flow (F) deposited in the SE depression (Fig. 17b).



772 **Fig. 18 – a) Wohletz (1983) diagram for the evaluation of the mechanical efficiency of the**
773 **products emitted in the form of Pyroclastic flows and fall/flow from Strombolian eruption**
774 **column collapse; b) products emitted by the 1538 eruption in the first eruptive phase as wet**
775 **pyroclastic flow, which buried the upper part of the Serapeum columns (above 8.2 m of height);**
776 **c) deposits of pyroclastic flow directed towards Pozzuoli, showing a thickness of about 5 m, in**
777 **the tunnel of the new road to Arco Felice**

778

779 According to the chronicles, on October 6th there was a new eruptive phase and 24 incautious visitors
780 died, surprised by the resumption of eruptive activity, which revealed itself with different
781 characteristics, mainly magmatic, that is, with a low water-magma interaction ratio (point b in Fig.
782 18a). In the hydromagmatic-magmatic transition, the eruptive cloud took the characteristic
783 ‘cauliflower’ shape of Strombolian eruptions, with a height of about 4 km, which, driven by winds
784 from the NW and then from the N, distributed the scoriaceous products towards the SE in the direction
785 of Nisida and the Neapolitan coast, then towards the S, in the direction of Bacoli and Capo Miseno
786 (Parascandola, 1943). The scoriaceous products of the second Strombolian magmatic eruptive phase
787 uniformly covered the basal units that formed the volcanic edifice during the first phase, with an
788 average thickness of about 0.5 m. The final phase of the eruption occurred with the collapse of the
789 Strombolian eruption column, which deposited a scoria flow in a depression on the eastern side of the
790 underlying cone of materials formed by phreatomagmatic pyroclastic flow units (Fig.17b). Overall,
791 the eruptive event of 1538, with the emission of 0.03 km³ of pyroclastic material, can be classified
792 with a VEI = 2.

793

794 **6. The seismicity before and after the 1538 eruption**

795

796 The main precursors of the eruption, as reported by chronicles, were the earthquakes. Earthquake
797 sequences preceded, accompanied and followed the 1538 event. In this context, seismic precursors
798 may depend on the occurrence of stress perturbation, determined by the arrival of magmatic gases, as
799 well as directly by magma intruded at shallow crustal levels (typically at depth of 3-4 km), originating
800 from the main reservoir located at about 7.5-8.0 km depth.

801 We analyze here the earthquake sequences that occurred before the eruption. Earthquake magnitudes,
802 from inferred intensities of these earthquakes, have been computed as described in the Appendix 3.
803 We can then compare past earthquakes with those occurred during the recent unrests.

804

805 **6.1 The seismic phases that accompanied the ground uplift and the eruption**

806 We can classify the earthquake sequences into long-term, medium-term and short-term precursors.
807 - The *long-term seismic precursors* started in 1448. Intense seismicity in 1468 - 1470 ($I_o = VII$,
808 Mercalli scale) (Guidoboni and Ciuccarelli, 2011; Francisconi et al., 2019) (Fig. 19a – interval A),
809 culminated with vigorous fumarolic-hydrothermal activity at Solfatara, 2 km NE of Pozzuoli, that
810 caused widespread damage to the vegetation in surrounding areas. This may indicate a broadening of
811 the area affected by intense degassing (Francisconi et al., 2019). Another seismic phase was reported
812 in 1475 (Guidoboni, 2020), with maximum intensity $I_o = IV - V$, followed by accelerating ground
813 uplift for the next 20 years. This period ended with a strong seismic phase in October 1498, reaching
814 a maximum intensity $I_o = VII$. Low-intensity seismicity then followed from 1499 to 1503 (maximum
815 intensity $I_o = V$) (Fig. 19a – interval A). Such a long-term precursory phase can be attributed mainly
816 to degassing from the deep magma chamber increasing pressure in the shallow layers of the
817 geothermal system, without requiring a significant contribution from magma intrusion at shallow
818 depth.

819 *Medium-term precursors* emerged with seismic events in 1505 and 1508, of higher intensity than
820 before (maximum intensity $I_o = VIII$) (Guidoboni and Ciuccarelli, 2011). Faster ground uplift resulted
821 in serious damage to buildings and caused several casualties. This seismic phase could have been
822 caused by either a higher stress associated with increasing pressure and uplift, or magma intrusion
823 from the deep magma chamber into shallower levels. This intrusion could have produced higher
824 stress resulting in seismic activity of greater intensity. Although it is obviously difficult to identify,
825 from historic sources alone, the respective roles of the deep degassing into the hydrothermal system
826 versus shallow magma intrusion, we believe that the reported evidence of vegetation damage and
827 increased degassing in the first phase, and the increase of earthquake intensity in the second phase,
828 indicate respectively a main contribution of degassing perturbing the hydrothermal system, in the first
829 phase, and of shallow magma intrusion in the second phase. This phase ended in 1520, with a medium
830 intensity earthquake ($I_o = V-VI$) (Fig. 19a – interval B)..
831
832

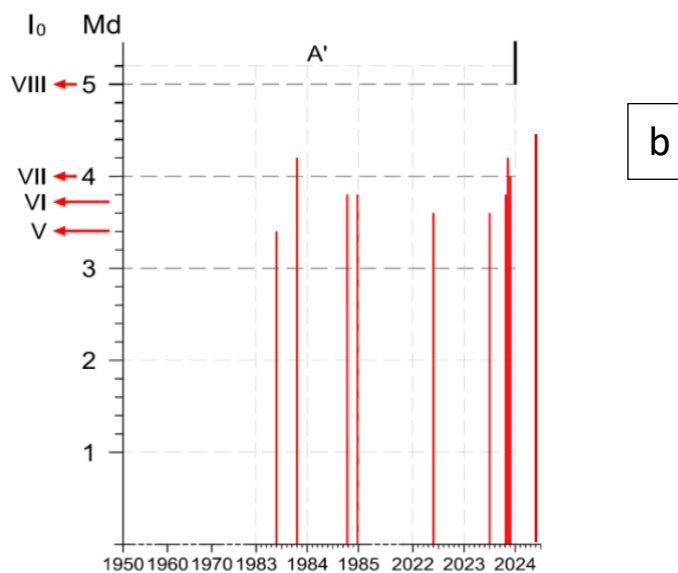
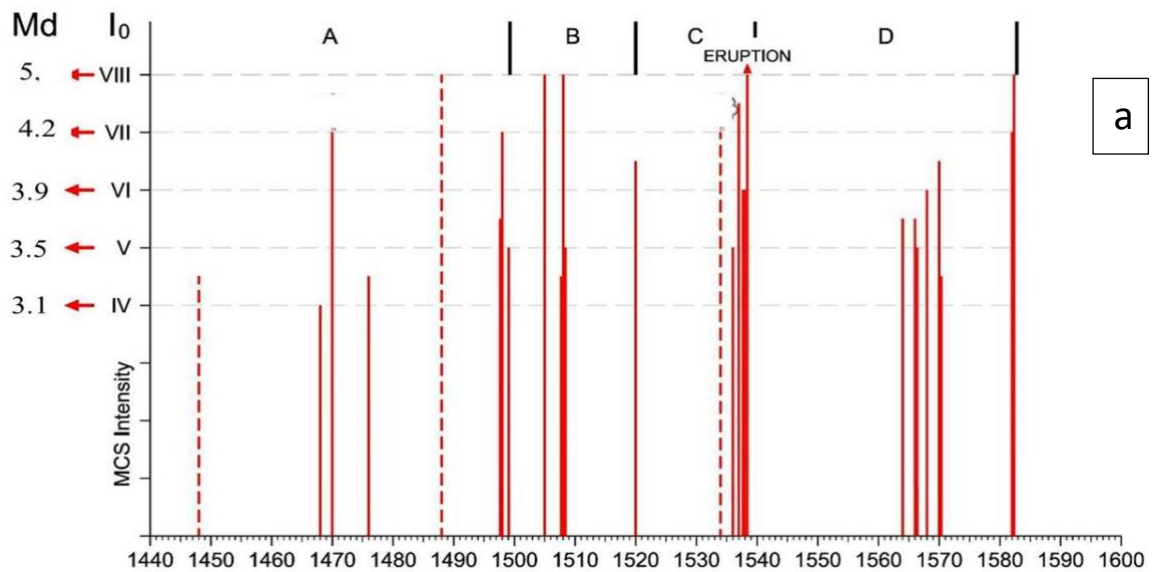


Fig. 19 – a) Reported earthquakes occurred before and after the 1538 eruption (after Guidoboni and Ciuccarelli, 2011). The computed intensities of these earthquakes have been converted in magnitudes using the considerations made in the appendix 3. b) Highest magnitude earthquakes ($M \geq 3.5$) occurred since 1950 to present.

After 16 years of relative seismic quiescence, possibly characterized by low-intensity earthquakes not reported in chronicles, a short-term precursory phase began in 1536. It started with continuous seismicity, without major damage ($I_0 = \text{III} - \text{IV}$), continuing with similar features until the early 1537. It is possible that this last seismic phase, characterized by relatively low magnitude, was caused by low-frequency seismicity, resulting from magma oscillations during the fractures opening (see Chouet, 1996). This seismicity became more frequent just before the eruption. In February of the same year, the seismic activity peaked with stronger events ($I_0 = \text{VI} - \text{VII}$), accompanied by an

847 increase in the fumarolic activity at Solfatara. This provides evidence that this seismicity could be
848 again related to perturbations in the hydrothermal system. A final increase in seismic activity ($I_o =$
849 VIII), began in mid-June 1538, accompanied by a localized, significant additional ground uplift at
850 the eruption site, located 3 km away from the center of previous maximum uplift (Fig. 19a – interval
851 C) (Parascandola, 1943, Rolandi et al., 1986; Guidoboni and Ciuccarelli, 2011; Guidoboni, 2020).

852

853 **6.2 The post-eruption seismicity**

854 We will now consider the seismic phase following the eruption just described, which we will indicate
855 as the *aftereffect of the 1538 eruption*.. It began in 1564 with earthquakes of medium intensity ($I_o =$
856 V - VI), followed by a phase of lower intensity 2 years later. In 1570 seismic intensity increased (I_o
857 = VI - VII), causing damage to the buildings of the city of Pozzuoli. Between 1575 and 1580 a new
858 phase of low seismic intensity began, culminating, in 1582, with two earthquakes, respectively of
859 intensity $I_o = VII - VIII$. These earthquakes caused partial collapses in several houses and serious
860 damage to churches and buildings, as well as numerous casualties (Parascandola, 1943; Guidoboni e
861 Cucciarelli, 2010; Guidoboni, 2020).

862

863 **7. Comparison of precursory phases of 1538 eruption with current unrest**

864 Our reconstruction of historical ground movement and seismicity has identified features common to
865 the medieval and present unrest. The main similarity is that the seismicity, has been clearly correlated
866 both with the total uplift and the uplift rate and it is practically absent in periods of subsidence (Dvorak
867 and Gasparini, 1991; Kilburn et al., 2017; Troise et al., 2019). We found, in particular, that seismicity
868 of period 1950-2024 is on the same order than the period 1430-1503, whereas the latter, as we have
869 previously observed, was the first phase of preparation before the 1538 eruption. Although the ca. 10
870 m of total amount of uplift in the period 1430-1503 was more than double than the total uplift recorded
871 since 1950-2024, of about 4.3 m., the seismicity in the two periods has been remarkably comparable.
872 The maximum magnitude, $M=4.6$ recently occurred on March 13th, 2025, is in fact very similar to the
873 maximum magnitude reconstructed for the period 1430-1503 (Fig.19a interval A and Fig.19b interval
874 A').

875 It is also interesting to compare the average uplift rate before the 1538 eruption with that observed
876 since 1950 to present. In particular, we can compare the average uplift rate occurred in the first 70-
877 73 years, since 1430 to 1503, with that observed since 1950 till now. In the period 1430-1503
878 maximum ground uplift was about 10 m, thus implying an average uplift rate of about 13.5 cm/year;
879 actually, the average ground uplift since 1950 has been less than half, at 6.1 cm/year, although
880 since 1983 To 1984 it has been increasing to about 12-20 cm/year.

881 Another common feature is that both seismic phases, as well as ground uplift, can be likely ascribed
882 to the effect of pressurized hydrothermal fluids (Moretti et al., 2017; 2018; Troise et al., 2019). So,
883 till now there is a close analogy between the ‘long term precursory phase’ preceding the 1538 eruption
884 and the recent unrest 1950-2023; the only clear difference is, as we already noted, the much lower
885 cumulative uplift (and consequently average uplift rate) of the recent unrest.
886 Such observations led us to consider two possible scenarios for the evolution of the present unrest.

887

888 **7.1 First scenario**

889 The first scenario would imply that the present unrest progresses towards a new eruption. Although
890 there is, presently, no evidence for shallow magma intrusions occurring during the present unrest
891 since 2006 (see Moretti et al., 2017, 2018; Troise et al., 2019; Lima et al., 2024) a new shallow magma
892 intrusion, in the near future, cannot be ruled out. Another possibility is that the mush, which should
893 be present at low depth, could be re-mobilised by hot fluids coming from the main magma chamber,
894 the way we explained in the previous paragraphs. Troise et al. (2019), showed in fact evidence for a
895 likely shallow magma intrusion occurred at about 3 km of depth, during the 1982-1984 unrest, with
896 a volume of about 0.03 km³, i.e. the same order of magnitude of the erupted volume in the 1538 event.
897 The same authors calculated, in agreement with other authors (Woo and Kilburn, 2010; Moretti et al.,
898 2013; Moretti et al., 2018), that such a sill intrusion should have become like mush, after about 20
899 years, i.e. around 2003. If the actual unrest will progress towards an eruption, it is also very likely
900 that seismicity will increase, in frequency and magnitude, possibly reaching magnitudes around 5 or
901 even higher. Earthquakes of magnitude 5, in this area, would occur at very shallow depths (not higher
902 than about 3 km), so producing high intensities (higher than VIII MCS, see Fig. 19). Finally, from a
903 civil protection perspective, we must also take into account the possible onset of a post-eruptive
904 seismic phase, which after the 1538 eruption lasted more than about 40 years. In conjunction with the
905 prefigured scenario, the problem of forecasting the position of a new eruptive vent is also extremely
906 relevant because, in principle, it could be opening in any sector of the caldera. We believe that a
907 reliable indication of the most likely future vent could come from the most seismic areas, because
908 they reflect the areas of maximum shear stress. In this perspective, the Solfatara-Agnano area (see
909 Fig. 15a), which is by far the most seismically active one, could be the most probable site for future
910 vent opening. This area, which is also located on the main ring faults bordering the resurgent block,
911 is however also indicated as one of the most likely by probabilistic studies (Alberico et al., 202; Selva
912 et al., 2011). Anyway, the most effective way to address this problem would be the prompt
913 determination of localized uplift in addition to the usual bell-shaped one centered on Pozzuoli harbor.
914 Although some recent eruptions (e.g. at Hekla volcano: Wonderman, 2000) show that the rise of

915 magma from several km to the surface can be so fast to be practically useless for civil protection
916 purposes, localized and considerable ground uplift at the future eruptive vent was actually observed
917 before the 1538 eruption, making it likely that this precursor will be observed before a future eruption
918 in the area.

919 We must however consider the possibility that, even without new shallow magma intrusions, the
920 increase of pressure for aquifer heating above the critical threshold could produce a phreatic eruption.
921 Phreatic eruptions are in general very difficult to forecast, and also to detect from the past geological
922 record. However, there is some robust indication for at least one phreatic eruption occurred in the
923 area, in 1198 (Scandone et al., 2010); it is also realistic that most of the phreatomagmatic eruptions
924 in the area started as phreatic eruptions, as explained in previous paragraphs. The phreatic scenario
925 deserves maximum attention for the current evolution of the CF unrest, because of its serious
926 implications for civil defense purposes, and for the even higher difficulty to be forecasted, with
927 respect to a magmatic eruption.

928

929 **7.2 Second scenario**

930 As an alternative scenario, we should consider the one which stops sometimes without evolving
931 towards an eruption. Despite the similarity of the recent unrest with the first phase leading to the 1538
932 eruption, we could in fact consider the notable difference in the cumulative uplift between the past
933 and present unrests, in the first 73 years: 10 m from 1430 to 1503, as compared with less than 4.5 m
934 from 1950 to present. The level of ground uplift is critical, because it indicates the level of stress
935 accumulated underground. As pointed out by Kilburn et al. (2017), when the level of stress reaches a
936 critical value, the medium rheology becomes totally fragile and any small amount of incremental
937 stress can cause the collapse (i.e. the catastrophic fracturing) of the shallow crust, thus producing the
938 eruption. Actually, we don't know the critical stress level for the shallow crust at Campi Flegrei. The
939 very high deformation occurred before the 1538, namely 16 m plus the localized uplift occurred just
940 at the vent site before the eruption, seems to indicate that the critical stress level, at that time, may
941 have been much higher than the one presently reached. So, if it could be assumed the medium strength
942 today is similar, there is a possibility that the progression towards eruption conditions is too gradual
943 to culminate in an actual eruption, and the unrest may cease before reaching that point; or, however,
944 that the time to reach the critical stage will be much longer (200-250 years, instead of about 100).

945 **8. Conclusion**

946 In this paper, we have presented a detailed reconstruction of the ground deformation, and a
947 comprehensive analysis of the main observations characterizing the events before, during and after the

1538 Monte Nuovo eruption, the only eruption occurred at Campi Flegrei caldera in historical times. This reconstruction, based on clear historical evidence, has allowed us to correct some widely diffused but questionable reconstructions, found in the past and recent literature.. Specifically, we demonstrated that subsidence in the area began, at least, during the Greek colonization (VIII century BC) and persisted through Roman times, with documentation dating back to 90 BC. Additionally, we reconstructed the evolution of ground deformation at Pozzuoli harbor during the Middle Age, demonstrating that maximum subsidence occurred around 1430. We also tracked the ground level from 1430 until the first half of the 19th century, using historical data on the height of the Serapeum floor relative to sea level.

Furthermore, by reconstructing the subsidence and uplift of the Via Herculea, based on ancient chronicles, we provided clear evidence indicating that the local uplift preceding the eruption at the Monte Nuovo site, situated near Via Herculea, did not exceed 5-7 meters, since Via Herculea never re-emerged from sea before and during the eruption. This evidence disproves claims in recent literature (Di Vito et al., 2016), that suggested local uplift around M. Nuovo reached elevations as high as 19 m immediately before the eruption.

Our reconstruction of geophysical anomalies (mainly ground displacement and seismicity) preceding and following the 1538 eruption has been tentatively interpreted in comparison with observations and data collected during the recent unrests. This approach enables the formulation of two possible scenarios for the evolution of the present unrest, which, so far, has shown notable similarities to the long-term precursors of the 1538 eruption.

The first scenario involves the progression of phenomena towards an eruption, suggesting that, in the near future, earthquakes with magnitude up to 5 or slightly higher may occur, both preceding the eruption and persisting for several decades afterward. Conversely, the alternative scenario, implies that the unrest may cease before an eruption occurs. This possibility is supported by the fact that ground uplift observed from 1950 to 2024, compared with the uplift occurred over an equivalent period from 1430 to 1503, is significantly lower (4.3 m as compared to 10 m). Since the overpressure in the system is somewhat proportional to the amount of uplift, it is plausible that the recent unrest has not reached the critical value for catastrophic fracture of shallow rocks. In addition, if cumulative stress increases too slowly, a substantial amount of previous stress can be cleared depending on viscoelastic relaxation and its characteristic times. While the exact critical threshold and viscoelastic relaxation time remain unknown, they can be tentatively inferred from the maximum deformation observed before the 1538 eruption. The bell-shaped cumulative vertical displacement centered at Pozzuoli, before the 1538 eruption, was much larger, reaching 16 m., compared to the about 4.5 m recorded from 1950 to 2024. This substantial difference, assuming the rheology and strength of shallow rocks in the 0-3 km depth

982 range remain unchanged, would suggest that we are currently far from reaching the critical stress
983 threshold necessary for an eruption.

984 The main result, very important for its civil protection implications, this work underline is the strict
985 similitude between the pre-eruptive scenario leading to the 1538 eruption and the present unrest, started
986 in 1950 and still in progress. So, we should expect increasing seismic activity with seismic magnitudes
987 up to $M=5$, and a non-negligible probability of eruption in the next years or decades. In addition, we
988 have also shown that, as it occurred during 1538 eruption, even small eruptions, down to $VEI=2$, can
989 generate pyroclastic flows travelling several km on flat terrain. Finally, we want further to stress the
990 possibility of a phreatic eruption, which could likely be the starting phase of a phreato-magmatic one.

992 **Data availability**

993 All raw data can be provided by the corresponding authors upon request.

995 **Author contributions**

996 GR, GDN and CT analyzed historical and volcanological data; GDN and CT analyzed earthquake
997 intensity/magnitude data; MS analyzed seismic data; GR, MS and MDL wrote the manuscript draft
998 and prepared the figures; GDN, CT and MS reviewed and edited the manuscript.

1000 **Competing interests**

1001 The authors declare that they have no conflict of interest.

1003 **Acknowledgments**

1004 The authors want to thank Prof. Marina Petrone and Prof. Gioia Molisso who helped to recover some
1005 important Middle Age references on Campi Flegrei. Many thanks are also due to Christopher Kilburn
1006 and to another anonymous reviewer, who helped a lot to make the paper clearer.

1009 **References**

- 1010 Acocella V., 2010. Evaluating fracture patterns within a resurgent caldera: Campi Flegrei. Italy.
1011 Bull. Volcanol., 72, 623-638.
- 1012 Acocella V., 2019. Bridging the gap from caldera unrest to resurgence. Front. Earth Science, 7, 173.
1013 <https://doi.org/10.3389/feart.2019.00173>.

- 1014 AGIP, 1987. Geologia e geofisica del sistema geotermico dei Campi Flegrei. Servizi Centrali per
1015 l'Esplorazione, SERG-MMESG, San Donato
- 1016 Alberico, I., Petrosino, P., and Lirer, L., 2011. Volcanic hazard and risk assessment in a multi-source
1017 volcanic area: the example of Napoli city (Southern Italy), *Nat. Hazards Earth Syst. Sci.*, 11, 1057–
1018 1070, <https://doi.org/10.5194/nhess-11-1057-2011>, 2011.
- 1019 Altaner, S., Demosthenous, C., Pozzuoli, A., Rolandi, G., 2013. Alteration history of Mount Epomeo
1020 Green Tuff and a related polymictic breccia, Ischia Island, Italy: Evidence for debris avalanche.
1021 *Bulletin of Volcanology* 75, 5, <https://doi.org/10.1007/s00445-013-0718-1>
- 1022 Amato, L. and Gialanella, C., 2013. New evidences on the Phlegraean bradyseism in the area of
1023 Puteolis harbour. Conference: Geotechnical Engineering for the Preservation of Monuments and
1024 Historic Sites. <https://doi.org/10.13140/2.1.2326.0482>
- 1025 Amoruso, A., Crescentini, L., Berrino, G., 2008. Simultaneous inversion of deformation and gravity
1026 changes in a horizontally layered half-space: Evidences for magma intrusion during the 1982–1984
1027 unrest at Campi Flegrei caldera (Italy). *Earth Planet. Sci. Lett.*, 272, 181–188.
1028 <https://doi.org/10.1016/j.epsl.2008.04.040>.
- 1029 Amoruso, A., Crescentini, L., Sabetta, I., 2014. Paired deformation sources of the Campi Flegrei
1030 caldera (Italy) required by recent (1980–2010) deformation history. *J. Geophys. Res.*, 119, 858–879.
1031 <https://doi.org/10.1002/2013JB010392>.
- 1032 Anecchino, R., 1931. Agnano, l'origine del nome e del lago. *Bollettino Flegreo*, 5.
1033
- 1034 Aster, R. and Meyer, R., 1988. Three-dimensional velocity structure and hypocenter distribution in
1035 the Campi Flegrei caldera, Italy. *Tectonophysics*, 149, 195–218
1036
- 1037 Aucelli, P.C. et al., 2020. Ancient Coastal Changes Due to Ground Movements and Human
1038 Interventions in the Roman Portus Julius (Pozzuoli Gulf, Italy): Results from Photogrammetric and
1039 Direct Surveys. *Water*, 12, 658. <https://doi.org/10.3390/w1203065>

1040 Bachmann, O., Bergantz, G.W., 2006. Gas percolation in upper-crustal silicic crystal mushes as a
 1041 mechanism for upward heat advection and rejuvenation of near-solidus magma bodies. *Journ.*
 1042 *Volcanol. and Geoth. Res.*, 149, 85-102
 1043

1044 Bachmann, O., Huber, C., 2016. Silicic mushes reservoirs in the Earth's crust. *American*
 1045 *Mineralogist*, 101, 11, 2377–2404. <https://doi.org/10.2138/am-2016-5675>
 1046

1047 Barberi, F., Corrado, G., Innocenti, F., Luongo, G., 1984. Phlegraean Fields 1982–1984: Brief
 1048 Chronicle of a Volcano Emergency in a Densely Populated Area. *Bull. Volcanol.*, 47-2, 175-185.

1049 Bergantz, G.W., 1989. Underplating and partial melting: implications for melt generation and
 1050 extraction. *Science* <https://doi.org/10.1126/science.245.4922.1093>

1051 Berrino, G., Corrado, G., Luongo, G., Toro, B., 1984. Ground deformation and gravity changes
 1052 accompanying the 1982 Pozzuoli uplift. *Bull. Volcanol.*, 44-2, 187–200.

1053 Bianchi, R., Coradini, A., Federico, C., Giberti, G., Lanciano, P., Pozzi, J.P., Sartoris, G., Scandone,
 1054 R., 1987. Modeling of surface deformation in volcanic areas: The 1970–1972 and 1982–1984 crises
 1055 of Campi Flegrei, Italy. *J. Geophys. Res.*, 92, B13, 14139–14150. Brahm, R., Parada,
 1056 M.A., Morgado, E.E., Contreras, C., 2015. Pre-eruptive rejuvenations of crystalline mush by
 1057 reservoir heating: the case of trachy-dacitic lavas of Quetupillán Volcanic Complex, Chile (39°30'
 1058 lat. S). *American Geophysical Union, Fall Meeting 2015*, abstract id. V43B-3122, Bibcode:
 1059 2015AGUFM.V43B3122B
 1060

1061 Burgisser, A., Bergantz, G.W., 201. A rapid mechanism to remobilize and homogenize crystalline
 1062 magma bodies. *Nature* 471(7337):212-5, <https://doi.org/10.1038/nature09799>
 1063

1064 Battaglia, J., Zollo, A. Virieux, J., Dello Iacono, D., 2008. Merging active and passive data sets in
 1065 travelttime tomography: The case study of Campi Flegrei caldera (Southern Italy) *Geophysical*
 1066 *Prospecting*, 56, 555–573 <https://doi.org/10.1111/j.1365-2478.2007.00687.x>

1067 Bellucci, F., Woo, J., Kilburn, C. R. J. & Rolandi, G., 2006. In *Mechanisms of Activity and Unrest*
 1068 *at Large Calderas Vol. 269* (eds. Troise C., De Natale, G. & Kilburn, C.R.J.) *The Geological Society*
 1069 *of London Special Publication*, 141–158.

1070 Beauducel, F., De Natale, G., Obrizzo, F., Pingue, F., 2004. 3-D modelling of Campi Flegrei ground
1071 deformations: role of caldera boundary discontinuities. *Pure Appl. Geophys.*, 161.

1072 Boccaccio, G., 1355-1373. De Montibus.

1073 Bodnar, R. J., Cannatelli, C., de Vivo, B., Lima, A., Belkin, H.E., Milia, A., 2007. Quantitative model
1074 for magma degassing and ground deformation (bradyseism) at Campi Flegrei, Italy: implications for
1075 future eruptions, *Geology*, 35, 9, pp. 791–794.

1076 Calò, M., Tramelli, A., 2018. Anatomy of the Campi Flegrei caldera using enhanced seismic
1077 tomography models, *Scientific Reports*, 8, 1, 16254.

1078 Camodeca, G., 1987. Le antichità di Pozzuoli, la Ripa Puteolana e i resti sommersi del Porto Giulio,
1079 G. Macchiaroli Editore, Napoli.

1080 Cannatelli, C., Spera, F.J., Bodnar, R.J., Lima, A., De Vivo, B., 2020. Ground movement
1081 (bradysesim) in the Campi Flegrei volcanic area: a review. In: “Vesuvius, Campi Flegrei, and
1082 Campanian volcanism”, In: De Vivo B., Belkin H. E & Rolandi G., Eds, Elsevier, 15, 407-433. ISBN:
1083 978-0-128-16454-9.

1084

1085 Cappelletti, P., Petrosino, P., De Gennaro, M., Colella, A., Graziano, S.F., D’Amore, M., Mercurio,
1086 M., Cerri, G., De Gennaro, R., Rapisardo, G., Langella, A., 2015. The “Tufo Giallo della Via
1087 Tiberina” (Sabatini Volcanic District, Central Italy): a complex system of lithification in a pyroclastic
1088 current deposit. *Mineralogy and Petrology*, 109 (1) 85-101 [https://doi.org/10.1007/s00710-014-0357-](https://doi.org/10.1007/s00710-014-0357-z)
1089 [z](https://doi.org/10.1007/s00710-014-0357-z)

1090

1091 Carrara, A., Burgisser, A., Bergantz, G.W., 2020. The architecture of intrusions in magmatic mush.
1092 *Earth and Planetary Science Letters*, 549, 1, 116539.

1093 Caricchi, L., Annen, C., Blundy, J.D., Simpson, G., Pinel, V., 2014. Frequency and magnitude of
1094 volcanic eruptions controlled by magma injection and buoyancy. *Nature Geoscience*, 7, 126–
1095 130. <https://doi.org/10.1038/ngeo2041>.

1096 Caruso, M., 2004. Il territorio puteolano fra età romana e alto Medioevo. *Bollettino Flegreo*, Terza
1097 serie, N°17

1098 Cashman, K.V., Sparks, R.S.J., Blundy, J., 2017. Vertically extensive and unstable crystals mushes:
 1099 a unifying view of igneous processes associated with volcanoes. *Science* 355, 6331,
 1100 <https://doi.org/10.1126/science.aag3055>

1101 Charlton, D., Kilburn, C., Edwards, S., 2020. Volcanic unrest scenarios and impact assessment at
 1102 Campi Flegrei caldera, Southern Italy. *Journal of Applied Volcanology*, 9, 7 (DOI).

1103

1104 Chiodini, G., Vandemeulebrouck, J., Caliro, S., D'Auria, L., De Martino, P., Mangiacapra, A.,
 1105 Petrillo, Z., 2015. Evidence of thermal driven processes triggering the 2005-2014 unrest at Campi
 1106 Flegrei caldera. *Earth Planet. Sci. Lett.*, 414, 58-67. <https://doi.org/10.1016/j.epsl.2015.01.012>.

1107

1108 Chiodini, G., Caliro, S., Avino, R. et al., 2021. Hydrothermal pressure-temperature control on CO₂
 1109 emissions and seismicity at Campi Flegrei (Italy),” *Journal of Volcanology and Geothermal Research*,
 1110 414, 107245. <https://doi.org/10.1016/j.jvolgeores.2021.107245>.

1111

1112 Chouet, B. A. (1996). Long-period volcano seismicity: its source and use in eruption
 1113 forecasting. *Nature*, 380, 6572, 309-316. <https://doi.org/10.1038/380309a0>

1114

1115 Cinque, A., Rolandi, G., Zamparelli, V., 1983. L'estensione dei depositi marini olocenici
 1116 nei Campi Flegrei in relazione alla vulcanotettonica. *Boll. Soc. Geol. It.*, 104, 327-348

1117

1118 Colletta, T., 1988. Pozzuoli, città fortificata in epoca vicereale - Storia dell'Urbanistica/Campania 1-
 1119 Pozzuoli. Pubblicazione semestrale diretta da E. Guidoni. Supplemento Luglio-Dicembre

1120

1121 Costa, A., Di Vito, M.A., Ricciardi, G.P., Smith, V. C., Talamo, P., 2022. The long and intertwined
 1122 record of humans and the Campi Flegrei volcano (Italy). *Bulletin of Volcanology*, 84, 5.
 1123 <https://doi.org/10.1007/s00445-021-01503->

1124 D'Antonio, M., Civetta, L., Orsi, G., Pappalardo, L., Piochi, M., Carandente, A., De Vita, S.,
 1125 Di Vito, M.A., Isaia, R., 1999. The present state of the magmatic system of the Campi Flegrei
 1126 caldera based on a reconstruction of its behavior in the past 12 ka. *J. Volcanol. Geotherm.*
 1127 *Res.*, 91, 2-4, 247-268.

1128 De Jorio, A., 1820. Ricerche sul Tempio de Serapide in Pozzuoli, Monumenti inediti di Antichità e
 1129 Belle Arti, Napoli.

1130 Del Gaudio, C., Aquino, I., Ricciardi, G.P., Ricco, C., Scandone, R., 2010. Unrest episodes at Campi
 1131 Flegrei: A reconstruction of vertical ground movements during 1905–2009. Journal of Volcanology
 1132 and Geothermal Research 195, 1, 48-56. <https://doi.org/10.1016/j.jvolgeores.2010.05.014>

1133 De Natale, G., Zollo, A., 1986. Statistical analysis and clustering features of the Phlegraean Fields
 1134 earthquake sequence (May 1983-May 1984). Bull. Seism. Soc. Am., 76, 3, 801–814.
 1135 <https://doi.org/10.1785/BSSA0760030801>
 1136

1137 De Natale, G., Pingue, F., Allard, P. and Zollo, A., 1991. Geophysical and geochemical modeling of
 1138 the Campi Flegrei caldera. In '*Campi flegrei*' (G. Luongo R. Scandone eds.), J. Volcanol. Geotherm.
 1139 Res., 48, 199–222.
 1140

1141 De Natale, G., Pingue, F., 1993. Ground deformations in collapsed caldera structures. Journal of
 1142 Volcanology and Geothermal Research, 57, 1-2, 19-38.
 1143

1144 De Natale, G., Petrazzuoli, S.M., Pingue, F., 1997. The effect of collapse structures on ground
 1145 deformations in calderas. Geophysical Research Letters, 24, 1555–1558.
 1146

1147 De Natale, G., Troise, C., Pingue, F., 2001. A mechanical fluid-dynamical model for ground
 1148 movements at Campi Flegrei caldera. J. Geodyn., 32, 487-517.
 1149

1150 De Natale, G., Kuznetov, I., Krondrod, T., Peresan, A., Sarao, A., Troise, C., Panza, G.F., 2004.
 1151 Three decades of seismic activity at Mt. Vesuvius: 1972-2000. Pure Appl. Geophys., 161, 1, 123-
 1152 144. <https://doi.org/10.1007/s00024-003-2430-0>
 1153

1154 De Natale, G., Troise, C., Pingue, F., Mastrolorenzo, G., Pappalardo, L., Battaglia, M., Boschi, E.,
 1155 2006b. The Campi Flegrei caldera: Unrest mechanisms and hazards. (London: Geological Society)
 1156 Geol. Soc. London Spec. pub., 269, 1. <https://doi.org/10.1144/GSL.SP.2006.269.01.03>.
 1157

1158 De Natale, G., Troise, C., Mark, D., Mormone, A., Piochi, M., Di Vito, M.A., Isaia, R., Carlino, S.,
 1159 Barra., D., Somma, R., 2016. The Campi Flegrei Deep Drilling Project (CFDDP): New insight on
 1160 caldera structure, evolution and hazard implications for the Naples area (Southern Italy).
 1161 Geochemistry, Geophysics, Geosystem, <https://doi.org/10.1002/2015GC00618341>.
 1162
 1163 De Natale, G., Petrazzuoli, S., Romanelli, F., Troise, C., Vaccari, F., Somma, R., Peresan, A., Panza,
 1164 G.F., 2019. Seismic risk mitigation at Ischia island (Naples, Southern Italy): an innovative approach
 1165 to mitigate catastrophic scenarios. Eng. Geol., 261, 105285.
 1166
 1167 Di Bonito, R., Giamminelli, R., 1992. Le Terme dei Campi Flegrei, Topografia Storica. Jandi Sapi
 1168 Editori, Milano-Roma.
 1169
 1170 Di Girolamo, P., Ghiara, M.R., Lirer, L., Munno, R., Rolandi, G., Stanzione, D., 1984.
 1171 Vulcanologia e petrologia dei Campi Flegrei. Boll. Soc. Geol. Ital., 103.
 1172
 1173 Di Vito, M.A., Lirer, L., Mastrolorenzo, G., Rolandi G., 1987. The Monte Nuovo eruption (Campi
 1174 Flegrei, Italy). Bulletin of Volcanology 49, 608–615.
 1175
 1175 Di Vito, M.A., Isaia, R., Orsi, G., Southon, J., De Vita, S., D’Antonio, M., Pappalardo, L., Piochi,
 1176 M., 1999. Volcanism and deformations since 12.000 years at Campi Flegrei caldera
 1177
 1177 Di Vito, M.A., Arienzo, I., Braia, G., Civetta, L., D’Antonio, M., Di Renzo, V., Orsi, G., 2011. The
 1178 Averno 2 fissure eruption: a recent small-size explosive event at the Campi Flegrei caldera (Italy).
 1179 Bull. Volcanol 73:295–320. <https://doi.org/10.1007/s00445-010-0417>
 1180
 1180 Di Vito, M.A., Acocella, V., Aiello, G., Barra, D., Battaglia, M., Carandente, A., Del Gaudio, C., S.
 1181 de Vita, S., GP Ricciardi, G.P., Ricco, C., Scandone, R., Terrasi, F., 2016. Scientific Reports, 6,
 1182 Article number: 32245. <http://www.nature.com/articles/srep32245>
 1183
 1183 Dvorak, J.J. and Gasparini, P., 1991. History of earthquakes and vertical ground movement in Campi
 1184 Flegrei caldera, Southern Italy: comparison of precursory events to the A.D. 1538 eruption of Monte
 1185 Nuovo and of activity since 1968. Journ. Volc. Geoth. Res., 48, 1-2.
 1186
 1187 Dvorak, J.J., Mastrolorenzo, G., 1991. The mechanism of recent movements in Campi Flegrei
 1188 caldera, Southern Italy. Geologic Society of America special paper, 263.

1189 Druitt, T.H., Sparks, R.S.J., 1984. On the formation of calderas during ignimbrite eruptions. *Nature*,
1190 310, 679-681.

1191 Edmonds, M., Cashman, K. V., Holness, M., Jackson, M., 2019. Architecture and dynamics of
1192 magma reservoirs. *Phil. Trans. Royal Soc., Mat. Phis. and engeener. Sci.*, 377, 2139.
1193 <https://doi.org/10.1098/rsta.2018.0298>

1194

1195 Folch, A., Gottsmann, J., 2006. Faults and ground uplift at active calderas, Geological Society,
1196 London, Special Publications, 269, 109–120.

1197

1198 Fournier, R.O., 1999. Hydrothermal processes related to movement of fluid from plastic into brittle
1199 rock in the magmatic epithermal environment, *Econ. Geol.*, 94, 8, 1193-1211.

1200

1201 Francisconi, G., Todesco, M., Ciuccarelli, C., 2019. Storia del Monte Nuovo. L'ultima eruzione dei
1202 Campi Flegrei. INGV Vulcani.

1203

1204 Franco, E., 1974. La zeolitizzazione naturale: in zeoliti e zeolitizzazione. *Atti Convegni Licei*, 33-60

1205

1206 Fuiano, M., 1951. Niccolò Jamsilla. *Atti dell'Accademia Pontaniana. Nuova serie, Volume 3 – Anno*
Accademico 1949 -50 – Napoli - Stabilimento tipografico Giannini

1207

1208 Gaeta, F.S., Peluso, F., Milano, G., Arienzo, I., 2002. A Physical Appraisal of A New Aspect of
1209 Bradyseism: The Mini-uplifts. *Journal of Geophysical Research Atmospheres* 108(B8)
1210 <https://doi.org/10.1029/2002JB001913>

1211

1212 Gianfrotta, P.A., 1993. Puteoli sommersa, in F. Zevi (a cura di), *Puteoli*: 115-124. Napoli, Banco di
Napoli.

1213

1214 Gudmundsson, A., 2012. Magma chambers: Formation, local stresses, excess pressures, and
1215 compartments. *Jour. Volcanol. Geoth. Res.*, <https://doi.org/10.1016/j.jvolgeores.2012.05.015>

1216

1217 Guidoboni, E., Ciuccarelli, C., 2011. The Campi Flegrei caldera: historical revision and new data on
1218 seismic crises, bradyseisms, the Monte Nuovo eruption and ensuing earthquakes (twelfth century
1582 AD), *Bulletin of Volcanology*, 73, 6, pp. 655-677, <https://doi.org/10.1007/s00445-010-0430-3>

- 1219 Guidoboni, E., 2020. Pozzuoli - terremoti e fenomeni vulcanici nel lungo periodo. a cura di AISI-
1220 Associazione Italiana di Storia dell'Ingegneria - VIII Convegno di Storia dell'Ingegneria, Napoli,
1221 Volume I
- 1222 Gretener, P.E., 1969. On the mechanics of the intrusion of sills. Canadian Journal of Earth Sciences,
1223 6, 6.
- 1224 Gauthier, V., 1912. Il Bradisismo Flegreo all'epoca ellenica. Rend. Real Accad. Sci, Fis. e Mat.
1225 Napoli, Serie III, Vol. XVIII, Anno LI, 91-94.
1226
- 1227 Iervolino, I., Cito, P., De Falco, M. *et al.*, 2024. Seismic risk mitigation at Campi Flegrei in volcanic
1228 unrest. Nat. Commun. 15, 10474. <https://doi.org/10.1038/s41467-024-55023-1>
1229
- 1230 Isaia, R., Vitale, S., Di Giuseppe, M.G., Iannuzzi, E., D'Assisi Tramparulo, F., Troiano, A., 2015.
1231 Stratigraphy, structure, and volcano-tectonic evolution of Solfatara maar-diatreme (Campi Flegrei,
1232 Italy). GSA Bulletin, 127, 9-10, 1485–1504. <https://doi.org/10.1130/B31183.1>
1233
- 1234 Johnson, E.R., Wallace, P.J., Cashman, K.V., Granados, H.D., Kent, A.J.R., 2008. Magmatic volatile
1235 contents and degassing-induced crystallization at Volcán Jorullo, Mexico: Implications for melt
1236 evolution and the plumbing systems of monogenetic volcanoes. Earth Plan. Sci. Lett., 269, 477
1237
- 1238 Kilburn, C.R.J., De Natale, G., Carlino, S., 2017. Progressive approach to eruption at Campi Flegrei
1239 caldera in southern Italy. Nature Communications, 8, 15312
- 1240 Kilburn, C.R.J., Carlino, S., Danesi, S., Pino, N.A., 2023. Potential for rupture before eruption at
1241 Campi Flegrei caldera, Southern Italy. Commun. Earth Environ., 4, 190.
1242 <https://doi.org/10.1038/s43247-023-00842-1>
- 1243 Lanzarin, O., 2021. Trugli dei bagni di Pozzuoli. Immagine e fortuna di due edifici termali antichi.
1244 <https://doi.org/10.17401/lexicon.33.2021-i>
- 1245 Lima, A., De Vivo, B., Spera, F.J. *et al.*, Bodnar, M., Milia, A., Nunziata, C., Belkin, H., Cannatelli,
1246 C., 2009. Thermodynamic model for uplift and deflation episodes (bradyseism) associated with
1247 magmatic-hydrothermal activity at the Campi Flegrei (Italy). Earth Sci. Rev., 97, 1-4, 44–58.

1248 Lima, A. Bodnar, R.J., De Vivo, B., Spera, F. J., Belkin, H.E., 2021. Interpretation of Recent Unrest
 1249 Events (Bradyseism) at Campi Flegrei, Napoli (Italy): Comparison of Models Based on Cyclical
 1250 Hydrothermal Events versus Shallow Magmatic Intrusive Events. *Geofluids*, 2000255.
 1251 <https://doi.org/10.1155/2021/2000255>.
 1252
 1253 Lima, A., Bodnar, R.J., De Vivo, B., Spera, F.J., Belkin, H.E., 2024. The “breathing” Earth at
 1254 Solfatara-Pisciarelli, Campi Flegrei, southern Italy (2005–2024): Nature’s attenuation of the effects
 1255 of bradyseism. *American Mineralogist*, 110 (5): 820–825. doi: [https://doi.org/10.2138/am-2024-](https://doi.org/10.2138/am-2024-9516)
 1256 [9516](https://doi.org/10.2138/am-2024-9516)
 1257
 1258 Luongo, G., Cubellis, E., Obrizzo, F., Petrazzuoli, S.M., 1991. The mechanics of the Campi Flegrei
 1259 resurgent caldera: a model. *Journ. Volcan. Geotherm. Res.*, 45, 3–4, 161-172.
 1260 Mancusi, F., 1987. Campi Flegrei. Sergio Civita Editore, Napoli.
 1261
 1262 Marti, J., Lopez, C., Bartolini, S., Becerrill, L., 2016. Stress control of monogenic volcanism: A
 1263 review. *Front. Earth Sci., Sec. Volcanology*, 4
 1264
 1265 Marturano, A., Esposito, E., Porfido, S., Luongo, G., 1988. Il terremoto del 4 Ottobre 1983
 1266 (Pozzuoli): Attenuazione dell’intensità con la distanza e relazione magnitudo-Intensità, zonazione
 1267 della città di Napoli. *Mem. Soc. Geol. It.*, 41, 941-948

1268

1269 Marsh, B.D., 1989. Magma chambers. *Ann. Rev. Earth Planet Sci.* 17, 439–474.
1270 <https://doi.org/10.1146/annurev.ea.17.050189.002255>

1271

1272 Milana, G., De Sortis, A., Rovelli, A., 2010. Contenuto in bassa frequenza nei terremoti vulcanici del
1273 Monte Etna e danneggiamento degli edifici. Fascicolo N.2: Progettazione Sismica, Sezione Articoli
1274

1275 Moretti, R., Orsi, G., Civetta, L., Arienzo, I., Papale, P., 2013. Multiple magma degassing sources at
1276 an explosive volcano. *Earth Planet. Sci. Lett.*, 367, 95-104.
1277 <https://doi.org/10.1016/j.epsl.2013.02.013>.

1278

1279 Moretti, R., De Natale, G., Troise, C., 2017. A geochemical and geophysical reappraisal to the
1280 significance of the recent unrest at Campi Flegrei caldera (Southern Italy). *Geochemistry,*
1281 *Geophysics, Geosystems*, <https://doi.org/10.1002/2016GC006569>

1282

1283 Moretti, R., Troise, C., Sarno, F., De Natale, G., 2018. Caldera unrest driven by CO₂-induced drying
1284 of the deep hydrothermal system, *Scientific Reports* G., 8, 1, 8309.

1285

1286 Morhange, C., Marriner, N., Laborel, J., Todesco, M., & Oberlin, C., 2006. Rapid sea-level
1287 movements and noneruptive crustal deformations in the Phlegrean fields caldera,
1288 Italy. *Geology*, [34\(2\)](https://doi.org/10.1130/G21894.1), 93–96. <https://doi.org/10.1130/G21894.1>

1289

1290 Nespoli, F. et al., 2023. A reduced-turbulence regime in the Large Helical Device upon injection
1291 of low-Z materials powders. Nucl. Fusion, 63 076001. <https://doi.org/10.1088/174-4326/acd465>

1292

1293 Niccolini, A., 1846. La gran terma puteolana. Napoli

1294

1295 Orsi, G., De Vita, S., Di Vito, M., 1996. The restless, resurgent Campi Flegrei nested caldera (Italy):
1296 constraints on its evolution and configuration. Journal of Volcanology and Geothermal
1297 Research, 74, 3, 179–214.

1298

1299 Orsi, G., Civetta, L., Del Gaudio, C., de Vita, S., Di Vito, M. A., Isaia, R., Petrazzuoli, S.M., Ricciardi,
1300 G.P., Ricco, C., 1999. Short-term ground deformations and seismicity in the resurgent Campi Flegrei
1301 caldera (Italy): an example of active block resurgence in a densely populated area. Journal of
1302 Volcanology and Geothermal Research, 91, 2, 415–451.

1303 Osservatorio Vesuviano, 2022. Bollettino Mensile Campi Flegrei 2022 06 (In Italian).
1304 [https://www.ov.ingv.it/index.php/monitoraggio-e-infrastrutture/bollettini-tutti/mensili-dei-vulcani-](https://www.ov.ingv.it/index.php/monitoraggio-e-infrastrutture/bollettini-tutti/mensili-dei-vulcani-della-campania/flegrei/anno-2022-2/1114-bollettino-mensile-campi-flegrei-2022-06/file)
1305 [della-campania/flegrei/anno-2022-2/1114-bollettino-mensile-campi-flegrei-2022-06/file](https://www.ov.ingv.it/index.php/monitoraggio-e-infrastrutture/bollettini-tutti/mensili-dei-vulcani-della-campania/flegrei/anno-2022-2/1114-bollettino-mensile-campi-flegrei-2022-06/file)

1306

1307 Parascandola, A., 1943. Il Monte Nuovo ed il Lago Lucrino, in Bollettino della Società dei Naturalisti
1308 in Napoli, Volumi 1944–1946, 55, 151-312. Stab. tip. G. Genovese

1309

1310 Parascandola, A., 1947. I Fenomeni Bradisismici del Serapeo di Pozzuoli. Stabilimento Tipografico
1311 G. Genovese, Napoli.

1312

1313 Parmigiani, A., Huber, C., Bachmann O., 2014. Mush microphysics and the reactivation of crystal-
1314 rich magma reservoirs. JGR, <https://doi.org/10.1002/2014JB011124>

1315

1316 Pasquarè, G., Poli, S., Venzolli L., Zanchi A., 1988. Continental arc volcanism and tectonic setting
1317 in central Anatolia. Tectonophysics, 146, 217-230

1318 Rolandi, G., D'Alessio, G., Di Vito, M. (1985). Il sollevamento del suolo durante la fase preeruttiva
1319 del Monte Nuovo (Campi Flegrei). Rend. Acc., Sc. Fis. e Mat. in Napoli, 4, 52, 15 - 34

1320 Rolandi, G., Bellucci, F., Heitzler, M.T., Belkin, H.E., De Vivo, B., 2003. Tectonic controls on the
1321 genesis of the ignimbrites from the Campanian volcanic zone, southern Italy. In 'Ignimbrites of the

1322 Campanian Plain' Spec. Issue, B. De Vivo and R. Scandone Eds., Mineralogy and Petrology, 79, 3–
 1323 31

1324 Rolandi, G., De Natale G., Kilburn, C.R.J. et al., 2020a. The 39 ka Campanian Ignimbrite eruption:
 1325 new data on source area in the Campanian Plain,” in Vesuvius, Campi Flegrei, and Campanian
 1326 volcanism, Chapt. 8, B. Vivo, H. E. Belkin, and G. Rolandi, Eds., pp. 175–205, Elsevier

1327 Rolandi, G., Di Lascio, M., Rolandi, R., 2020b. The Neapolitan Yellow Tuff eruption as the source
 1328 of the Campi Flegrei caldera. in Vesuvius, Campi Flegrei, and Campanian volcanism, Chapt. 11, B.
 1329 Vivo, H. E. Belkin, and G. Rolandi, Eds., pp. 273–296, Elsevier.

1330 Rosi, M., Sbrana, A., (Eds.) 1987. Phlegrean fields (Vol. 9). Consiglio nazionale delle ricerche.
 1331

1332 Russo Mailer, C., 1979. La tradizione Medioevale dei bagni flegrei. Puteoli, studi di storia antica, III,
 1333 141-153

1334 Sabetta, F., Paciello, A., 1995. Valutazione della pericolosità sismica. La geologia di Roma- Memorie
 1335 descrittive della carta geologica d'Italia.

1336 Sacchi, M., Pepe, F., Corradino, M., Insinga, D.D., Molisso, F., Lubritto C., 2014. The Neapolitan
 1337 Yellow Tuff caldera offshore the Campi Flegrei: stratal architecture and kinematic reconstruction
 1338 during the last 15 ky. Mar. Geol. 354, 5-33

1339 Sacchi, M., Passaro, S., Molisso, F., Matano, F., Steinmann, L., Spiess, V., Pepe, F., Corradino, M.,
 1340 Caccavale, M., Tamburrino, S., Esposito, G., Vallefucio, M., Ventura, G., 2020a. The Holocene
 1341 marine record of unrest, volcanism, and hydrothermal activity of Campi Flegrei and Somma
 1342 Vesuvius. In: B. De Vivo, H.E. Belkin and G. Rolandi (Eds.) Vesuvius, Campi Flegrei, and
 1343 Campanian Volcanism, Elsevier Inc., Amsterdam, 435-469;
 1344 <https://doi.org/10.1144/GSL.SP.2006.269.01.0310.1016/B978-0-12-816454-9.00016-X>.
 1345

1346 Sacchi, M., Matano, F., Molisso, F., Passaro, S., Caccavale, M., Di Martino, G., Guarino, A., Innangi,
 1347 S., Tamburrino, S., Tonielli, R., Vallefucio, M., 2020b. Geological framework of the Bagnoli–
 1348 Coroglio coastal zone and continental shelf, Pozzuoli (Napoli) Bay. Chem. Ecol., 36, 529–549.
 1349

1350 Scandone, R., D'Amato, J., Giacomelli, L., 2010. The relevance of the 1198 eruption of Solfatara in
1351 the Phlegraean Fields (Campi Flegrei) as revealed by medieval manuscripts and historical sources.
1352 Journ. Volcanol. Geoth. Res., 189, 1–2, 202–206.

1353 Scarpa, R., Bianco, F., Capuano, P., Castellano, M., D'Auria, L., Di Lieto, B., Romano, P., 2022.
1354 Historic unrest of the Campi Flegrei caldera. In *Campi Flegrei. A Restless Caldera in A Densely*
1355 *Populated Area* (eds Orsi, G., D'Antonio, M. & Civetta, L.), 257–282.

1356 Selva, J., Orsi, G., Di Vito, M., Marzocchi, W., Sandri, L., 2011. Probability hazard map for future
1357 vent opening at the Campi Flegrei caldera, Italy. Bull. Volcanol., [https://doi.org/10.1007/s00445-011-](https://doi.org/10.1007/s00445-011-0528-2)
1358 [0528-2](https://doi.org/10.1007/s00445-011-0528-2) 1-0528-2.

1359 Somma, R., Iuliano, S., Matano, F., Molisso, F., Passaro, S., Sacchi M., Troise C., De Natale, G.,
1360 2016. High-resolution morphobathymetry of Pozzuoli Bay, southern Italy. Journ. Maps, 12, 222–
1361 230, <https://doi.org/10.1080/17445647.2014.1001800>.

1362 Soricelli, G., 2007. Comunità orientali a Puteoli. Press. Univers., Rennes, 129–144,
1363 <https://doi.org/10.4000/books.pur.6714>

1364 Sparks, S.R.J., Sigurdsson, H., Wilson, L., 1977. Magma mixing: a mechanism for triggering acid
1365 explosive eruptions. Nature, 267, 315–318

1366 Shelly, D., Hurwitz, S., 2022. Yellowstone caldera chronicles, September 5. Yellowstone Volcano
1367 Observatory, USGS ([https://www.usgs.gov/observatories/yvo/news/water-released-crystallizing-](https://www.usgs.gov/observatories/yvo/news/water-released-crystallizing-magma-can-trigger-earthquakes-yellowstone)
1368 [magma-can-trigger-earthquakes-yellowstone](https://www.usgs.gov/observatories/yvo/news/water-released-crystallizing-magma-can-trigger-earthquakes-yellowstone))

1369 Smith, V.C., Isaia, R., Pearce, N.J.G., 2011. Tephrostratigraphy and glass compositions of post-15 kyr
1370 Campi Flegrei eruptions: implications for eruption history and chronostratigraphic markers. Quat.
1371 Sci. Rev. 30, 3638–3660

1372

1373 Steinmann, L., Spiess, V., Sacchi, M., 2016. The Campi Flegrei caldera (Italy): Formation and
1374 evolution in interplay with sea-level variations since the Campanian Ignimbrite eruption at 39 ka.
1375 Journ. Volcanol. Geoth. Res., 327, 361–374

1376

1377 Strabone, 1 century BC - 1 century AD. Rerum Geogr., book V, cap. 4–5

1378

1379 Talavera Montes, A.J., 2021. Eruzioni, sismi e bradisismo nei Campi Flegrei in epoca romana tra
 1380 fonti storiche ed evidenze archeologiche e geologiche. In: *Living with Seismic Phenomena in the*
 1381 *Mediterranean and Beyond between Antiquity and the Middle Ages*, Proceedings of Cascia (25-26
 1382 October, 2019) and Le Mans (2-3 June, 2021) Conferences. Edited by Compatangelo Soussignan R.
 1383
 1384 Troise, C., Pingue, F., De Natale, G., 2003. Coulomb stress changes at calderas: modeling the
 1385 seismicity of Campi Flegrei (Southern Italy). *J. Geophys. Res.*, 108, B6, 2292,
 1386 <https://doi.org/10.1029/2002JB002006>.
 1387
 1388 Troise, C., De Natale, G., Pingue, F., Obrizzo, F., De Martino, P., Tammaro, U., Boschi, E.,
 1389 2007. Renewed ground uplift at Campi Flegrei caldera (Italy): New insight on magmatic processes
 1390 and forecast, *Geophys. Res. Lett.*, 34, L03301, doi:10.1029/2006GL028545.
 1391
 1392 Troise, C., De Natale, G., Schiavone, R., Somma, R., Moretti, R., 2019. The Campi Flegrei caldera
 1393 unrest: Discriminating magma intrusions from hydrothermal effects and implications for possible
 1394 evolution. *Earth Sci. Rev.*, 188, 108-122, <https://doi.org/10.1016/j.earscirev.2018.11.007>.
 1395
 1396 Vanorio, T., Prasad, M., Patella, D., Nur, A., 2002. Ultrasonic velocity measurements in volcanic
 1397 rocks: Correlation with microtexture. *Geophys. Journ. Intern.*, 149, 1, 22-36,
 1398 <https://doi.org/10.1046/j.0956-540x.2001.01580.x>
 1399
 1400 Vanorio, T., Virieux, J., Capuano, P., Russo, G., 2005. Threedimensional seismic tomography from
 1401 P wave and S wave microearthquake travel times and rock physics characterization of the Campi
 1402 Flegrei Caldera. *J. Geophys. Res.*, 110, 1-14
 1403
 1404 Vanorio, T., Kanitpanyacharoen, W., 2015. Rock physics of fibrous rocks akin to Roman concrete
 1405 explains uplifts at Campi Flegrei. *Science*, 349, 617–621
 1406
 1407 Varriale, I., 2004. Costa Flegrea ed attività bradisismica dall'antichità ad oggi. In *Rotte e Porti del*
 1408 *Mediterraneo dopo la caduta dell'Impero Romano d'Occidente*. IV seminario, Genova 18-19 Luglio.
 1409 De Maria L. and Turchetti R. Eds.
 1410

- 1411 Vinciguerra, S., Trovato, C., Meredith, P.G, Benson, P.M., Troise, C., De Natale, G., 2006.
 1412 Understanding the Seismic Velocity Structure of Campi Flegrei Caldera (Italy): From the Laboratory
 1413 to the Field Scale. *Pure appl. geophys.*, 163, 2205–2221, <https://doi.org/10.1007/s00024-006-0118-y>
 1414
- 1415 Wohletz, K.H., Zimanowski, B., Büttner, B.R., 2013. Magma-water interactions. in *Modeling*
 1416 *Volcanic Processes: The Physics and Mathematics of Volcanism* (Fagents, S.A., Gregg, T.K.P.,
 1417 Lopes, R.M.C. eds.) 230–257. Cambridge University Press.
 1418
- 1419 Woods, W., Cowan, A., 2009. Magma mixing triggered during volcanic eruption. *Earth and Planetary*
 1420 *Science Letters*, 288, 1–2, 30, 132-137
- 1421 Woo, J.Y.L., Kilburn, C.R.J., 2010. Intrusion and deformation at Campi Flegrei, southern Italy: Sills,
 1422 dikes, and regional extension. *J. Geophys. Res.*, 115, B12210
 1423
- 1424 Wunderman, R. ed., 2000. Global volcanism Program. Report on Hekla (Iceland). *Bullettin of global*
 1425 *volcanism network*, 25:2. Smithsonian Institution. [https:// doi org/10.5470/si](https://doi.org/10.5470/si).
 1426
- 1427 Zollo, A., Maercklin, N., Vassallo, M., Dello Iacono, D., Virieux, J., Gasparini, P., 2008. Seismic
 1428 reflections reveal a massive melt layer feeding Campi Flegrei caldera, *Geophys. Res. Lett.*, 35,
 1429 L12306, doi:[10.1029/2008GL034242](https://doi.org/10.1029/2008GL034242).
 1430

1433 **Appendix 1 - Evolution of the vertical movements involving the Via Herculea**

1435 The following notes refer to the diagram represented in Fig. 3, reporting at each point the historical information
 1436 related to ground deformation in the Averno area:

- 1437
- 1438 **1-** The shoreline between the cities of Baia and Pozzuoli took on a new conformation with the natural building
 1439 of a sandy coastal bar after the eruptions of Averno and Capo Miseno (5 - 3.7 ka), the last of the second post-
 1440 calderic cycle. We remember that the name *Averno* derived from the Greek *Aornon*, that is *place without*
 1441 *birds*, in reference to the presence of post-volcanic sulphurous fumes that caused the death of the birds that
 1442 flew over the waters. The dark and gloomy appearance of the landscape led the ancients to consider it the
 1443 entrance to Hades, as reported by Virgil (*Aeneid*, VI, vv 350).
 1444 We do not know precisely the time of formation of the bar structure; we can only hypothesize that it was
 1445 probably positioned between the 18th and 17th centuries BC in the coastal stretch between the cities of Baia

1446 and Pozzuoli, with a height of about 6 m, like the other coastal bars formed more recently in nearby areas,
1447 where the seabed has a depth of about 6-7 m. The formation of the sea barrier blocked a portion of the sea
1448 inside the inlet, which took the shape of a lake (Fig. 2a and Fig. 4).

1449

1450 2- This point can be traced back, from a historical and chronological point of view to the 8th century BC. In
1451 the diagram it is positioned at approximately 5 m above sea level, suggesting a subsidence of the coastal bar
1452 of about 2 m from the previous point. In fact, from a writing by Diodorus Siculus (Book IV) we know that:..
1453 ***this dam was continually invaded and ruined by the stormy sea, which often made it impassable...*** It is known
1454 from coastal dynamics studies that waves breaking against a dam, placed above a seabed 7 m deep, reach a
1455 height equal to 3/4 of the depth of the same seabed, in this case approximately 5 m, i.e., a height equal to the
1456 barrier above the sea level. Therefore, the via Herculea, hit by violent waves, constituted an impassable road
1457 for the inhabitants of Cuma to reach the lands they cultivated in the surroundings of Pozzuoli, which, starting
1458 from the 8th century, took the name of Via Herculea (Fig. 2b and Fig. 4). Finally, the hypothesis of a height
1459 of 5 m, as resulting from submersion started since the 17th century BC, seems likely.

1460

1461 3- 4 - The body of water formed by the coastal bar, in the 1st century BC, was owned by Sergio Orata. The
1462 lake, making generous profits from fish farming, was named "*Lucrino*", derived from the Latin *Lucrum* (profit)
1463 (Fig. 2c). The owner, around 60 BC, to protect his interests turned directly to the Roman Senate to have the
1464 Via Herculea repaired, because at that time, being at a height of about 2 m above sea level, it had almost been
1465 destroyed by the waves that crossed it, preventing him from practicing his lucrative fish farming business
1466 (point 3). The Senate appointed Julius Caesar, who in 59 BC built a breakwater barrier, located outside the
1467 dam towards the open sea (*Opus Pilarum*). He also ordered the installation of canals closed by opening
1468 platforms (*Claustre*). Julius Caesar's project defended the Via Herculea essentially from the horizontal force
1469 exerted by violent wave motion, not understanding the effect of subsidence. In 37 BC, general Agrippa, by
1470 order of Octavian, engaged in the naval war against Pompeo Sextus, chose the coastal sector between the lakes
1471 Lucrino and Avernus for the construction of a new military port system, called *Portus Julius*. A new main
1472 entrance was built, consisting of a canal with two long banks in 'opus pilarum', cutting and equipping the Via
1473 Herculea with a mobile bridge, to access its interior, while at the same time widening the narrow opening that
1474 connected the Averno and Lucrino lakes to allow access of large ships in the shipyard (Fig. 2c). Furthermore,
1475 Agrippa reinforced the Via Herculea and added piers, supported by orthogonal pillars and having also sensed
1476 a problem of subsidence,... ***raised its level (Strabone, 1 century BC-1 century AD)*** (point 4).

1477

1478 5- 6 - The abandonment of Portus Julius by the Roman fleet, starting from 12 BC, as well as of the remaining
1479 part of Lake Lucrino, due to the impossibility of continuing fish farming, was the result of the continuing
1480 subsidence, which, according to Aucelli et al. (2020), between 37 BC and the beginning of the 1st century AD
1481 further accelerated.

1482 In the 5th century AD the dam, few meters above sea level (point 5), was also damaged by a violent sea storm.
1483 An attempt to restore the dam again was made by Theodoric, regent of the Ostrogothic kingdom in Italy from
1484 493 AD, who decided, in 496 AD, to repair the damage and probably also raised its level (*Cassiodorus, Varia,*
1485 *Book 1*) (point 6). This can be also deduced from the fact that Lake Lucrino was still well identified in 522
1486 AD (G.C. Capaccio - Puteolana historia, in Parascandola 1943).

1487

1488 **7-8** - Around the second half of the 6th century (556 AD), some fishermen attempted to reactivate fish farming
1489 in Lake Lucrino, but the dam soon could not guarantee an adequate yield, because it had reached a height of
1490 just a few meters above sea level (point 7), not allowing fish farming (Parascandola, 1943).

1491 As we will show in Appendix-2, historical documents indicate that, at the lower city around Pozzuoli, the
1492 famous Serapeo (Macellum) began the phase of submersion below sea level in the 4th-5th century AD. At the
1493 area facing the Avernus, the above historical documents indicate that the submersion most likely occurred
1494 between the 6th and 7th centuries AD. This could be related to either height increasing interventions and /or
1495 to a lower speed of subsidence at the site of Via Herculea, as compared to the Serapeo.

1496

1497 **9** – In the 14th century we have evidence of the submersion through the writings of Petrarca and Boccaccio.
1498 Below we will report some sentences from the two poets, giving indications on the subsidence in this period
1499 (Parascandola 1943):

1500 - Petrarca, who lived in Naples in 1341, visited the coastal area of Avernus, (*...I then saw the places of*
1501 *Avernus and Lucrino..... and the superb road of Gaius Caligula now swallowed up by the waves..... Note*
1502 *that Opus Pilarum mistakenly believed to be the road of Caligula*). From this observation we deduce that
1503 Opus Pilarum was submerged in the 14th century (Fig. A1). From the same observation it further seems likely
1504 that, since the 4-5 m high pylons, submerged for a couple of metres, are not visible, and given the pylons were
1505 higher than Via Herculea of about 3 meters, the already submerged Via Herculea should have been submerged
1506 at that time for about 5-6 m.

1507 - Boccaccio came to Naples in 1348 and, after visiting the Averno area, he clearly expressed the concept,
1508 although indirectly, that Lake Lucrino was not recognized as it was invaded by the sea, mixing with the waters
1509 of Avernus (*...to Avernus, connected in ancient times with the nearby lake Lucrino where it recalls the*
1510 *waters of portus Iulius*: Boccaccio, 1355-1373).

1511 Boccaccio noted that, since there was no barrier on the Via Herculea which formed the Lucrino, the rough sea
1512 even broke into Lake Averno. Therefore, we can undoubtedly say that in the 14th century via Herculea was
1513 completely submerged and Lake Lucrino disappeared because it was invaded by the sea.

1514

1515 **10** - As we will demonstrate later, in the 15th century the ground movements of the Campi Flegrei area changed
1516 from subsidence to uplift. The uplift began, the actual amount of which in the Averno area can be only given
1517 in an approximate but equally significant way, because it is ascertained, from the writings of all the chroniclers
1518 of the time (see Parascandola, 1943) that the Via Herculea did not re-emerge in this period (fig 2d). What is

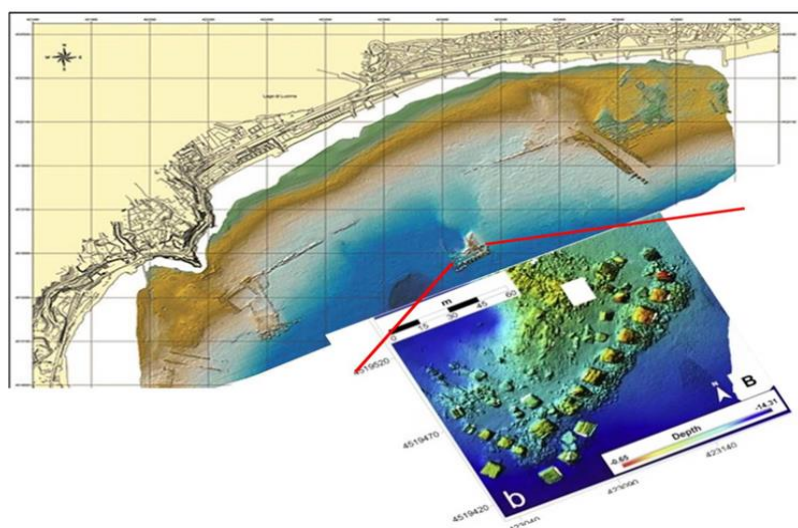
1519 reported by the historian San Felice is almost common to all the chroniclers: *The sea had taken possession of*
 1520 *Lucrino, so that the name could no longer be given to the ancient lake.*
 1521

1522

1523 **Fig. A1 - The remains of the Via Herculea currently located at 4-5m bsl, with the columns of Opus**
 1524 **Pilarum approximately 300m away in the open sea. An enlargement of the structure of Opus Pilarum is**
 1525 **also reported**

1526 Shortly before the eruption, the general caldera uplift was also accompanied by a localized uplift of the area
 1527 where Monte Nuovo would have risen shortly after, in 1538, located in close contact with the Lucrino basin
 1528 (Fig. 2d). Such a local uplift was estimated at about 7 m (Parascandola, 1943), so the Via Herculea would
 1529 certainly have emerged if it had been close to the sea surface at the end of the 15th century. A significantly
 1530 larger uplift, of 19 m as hypothesized by Di Vito et al (2016), can be certainly ruled out from the observation
 1531 that Via Herculea did not reemerge.

1532 The topic of the local uplift before eruption is relevant, so we insist on other aspects linked to the entire area
 1533 buried by the products of 1538 Monte Nuovo eruption. Until a short time before the eruptive event, two small
 1534 tuff hills, called *Montagnella* and *Monticello del Pericolo* (Parascandola, 1936), overlooked the Averno Bay,
 1535 above which the *village of Tripergole* extended. This village, thanks to the Angevins, developed with the
 1536 construction of a hospital with 30 beds, to access the numerous springs and thermal facilities available to the
 1537 hospitalized patients, with an adjoining pharmacy. Ancient buildings used for thermal baths (*Trugli*) present
 1538 in the Tripergole area were highly compromised between the end of the 15th century and the beginning of the
 1539 16th, when the Pozzuoli area was hit by major earthquakes. The earthquakes caused extensive damage to the
 1540 thermal health and ecclesiastical buildings of Tripergole, but not so devastating than expected if a ground uplift
 1541 about 20 m high would have occurred. Also the so-called *Temple of Apollo*, still present along the north-
 1542 eastern bank of the Averno lake (Fig. A2), testifies against a so large and sudden uplift. The structure is an
 1543 imposing building identified as a grandiose thermal room, covered by a dome, now partly collapsed, which
 1544 measured approximately 38 metres in diameter, built in the 1st century AD to exploit a series of hydrothermal



1545 springs along the eastern side of Avernus, then expanded with the large octagonal hall (the one that is still
1546 visible) in the following century. This structure was identified by Biondo da Forlì as the bathroom of Cicero
1547 (Lanzarin, 2021), that, due to its particular location protected by the Averno crater belt, was not involved in
1548 the burial of the *Monticello del Pericolo*, the *Montagnella* and the village of *Tripergole*, with its renowned
1549 thermal baths.

1550



1551

1552 **Fig. A2 – The so-called Temple of Apollo on the east bank of the Avernus. You can see the remains of a**
1553 **circular building with a "cap" vault, which later collapsed, typical of a "Truglio", i.e. a spa building**
1554 **(internet source)**

1555

1556 **Appendix 2 - Evolution of the ground movements involving the Pozzuoli area**

1557

1558 Phases of submersion during the Greek age have been detected in the Pozzuoli area by Gauthier (1912),
1559 specifically in the eastern sector of Agnano. The author discovered Greek walls beneath the ruins of Roman
1560 baths which were restored in the 6th century AD. These, in turn, underlie lacustrine sediments that filled an
1561 ancient lake originally existing within the Agnano crater. However, the most evident subsidence phases have
1562 been recorded since Roman times, by the structures of the so-called Temple of Serapis in Pozzuoli. Built in
1563 the 2nd century AD and restored and completed in the 3rd century AD, during the Severan era, this structure
1564 exhibits the typical architecture of a Roman market ("Macellum").

1565 To determine whether the construction preceding the 2nd century AD had a connection with a temple, we must
1566 go back to 105 BC, when a contract was stipulated between the municipality of Pozzuoli and a college of
1567 builders for repairs of public buildings (lex parieti faciundo). Among these was the Ades Serapis (Parascandola
1568 1947), indicating that a temple dedicated to Serapis, (an Alexandrian deity often regarded as protector of
1569 merchants and sailors) existed during this period. By the end of the 2nd century BC, the cult of Serapis had
1570 spread throughout the Mediterranean and its sanctuaries, as well as those of other Egyptian deities, were
1571 frequented by Roman-Italics. It is probable, therefore, that the introduction of the cult of Serapis in Puteoli is
1572 related to the presence of an Egyptian community in the Puteolan port (Soricelli 2007). It is important to try to

1573 establish the relationships between this building and the Macellum built later, specifically whether the Aedes
1574 Serapis could have an ancestral link with a more recent cult building, that was then transformed into a typical
1575 Roman market. This relationship is suggested by the discovery of a statue of Jupiter Serapis during the
1576 excavations of the Macellum in 1750 (see below). However, data reconstructed by Amato and Gialanella
1577 (2013; Fig.3), indicate that the first floor present in the substrate below the Macellum dates from the Flavian
1578 period (69 -96 AD). The finds in the reworked pyroclastic materials which are 4 meters thick below the first
1579 floor indicate a chronological interval between the end of the Republic and the beginning of the Empire (44
1580 BC - 14 AD). This suggests that the Aedes Serapis was likely built in a different position from the macellum,
1581 with which it therefore has no ties. The architectural elements of Macellum are part of the restoration works
1582 carried out on the Serapeum during the Severan Age (194 - 235 AD), with the installation of the 4th floor around
1583 230 AD, located approximately 2 m above the 3rd floor. The existing structure (Fig. 6), still present in the
1584 same area today, provides important evidence for reconstructing the ground movements. These movements
1585 can be identified in:

1586 *The marble floor of the macellum (4th floor; see also Fig. A3b);

1587 * The height of the three columns of the pronaos (12.70 m high, with the first 6.2 m displaying a 2.70m band
1588 perforated by lithophagus colonies (Fig. A3).

1589 The historical information about the ground movements, is schematized in Fig. 6 of the main text, as follows:

1590 **1** - In the 2nd century AD the 3rd floor of the Serapeum reached approximately 1m above sea level. It was
1591 sporadically invaded by the sea, to the point that, it was considered appropriate to build a 4th floor in 230 AD,
1592 located at 2m above sea level.

1593

1594 **2** - The flooding progressively affected the coast, leading to the transfer of ships from the port of Puteoli to
1595 Constantinople in 325-330 AD (Gianfrotta 1993). It is important to highlight that the 4th floor was invaded
1596 by the sea in 394 AD. The bank was restored on the left side and the right side of the macellum, in the area
1597 where structures functional to the port and the emporium were located, and to protect it from the sea waves
1598 with the construction of coastal embankments. These important works were supervised by the Campanian
1599 Consul Valerius Hermonius Maximus (Camodeca 1987, Caruso 2004).

1600

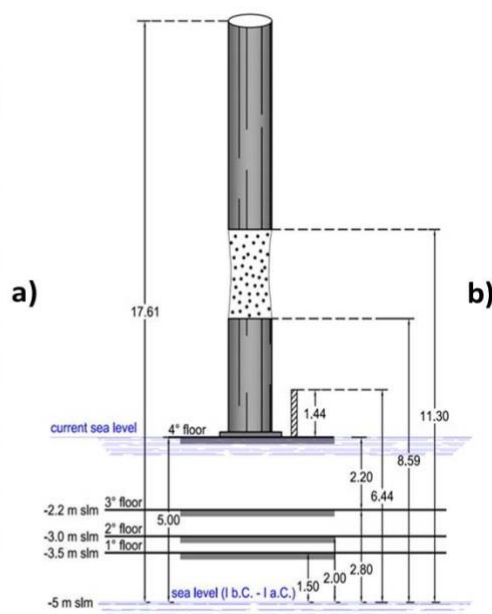


Fig. A3 – a) Macellum showing pronao columns, b) Floors underlying columns

1601

1602

1603

1604 **3** - In the 6th-7th century, the citizens who had completely depopulated the lower part of Pozzuoli felt the need
 1605 to take refuge in a sort of fortified citadel (castrum), equipped with a drawbridge, giving rise to the Acropolis
 1606 of the Rione Terra (Varriale, 2004).

1607

1608 **4** - In the 9-10th century, according to Parascandola (1947), the maximum submersion of the 4th floor of the
 1609 Serapeum occurred. Due to the subsidence of the Pozzuoli area, between the 8th and 10th centuries, the Agnano
 1610 Plain, immediately east of Pozzuoli, was invaded by water for the stagnation of thermal and rainwater,
 1611 transforming it into a lake (Annechino, 1931).

1612

1613 **5 -7** - In such a context, the most critical periods of the submersion phase occurred. The sea increasingly
 1614 surrounded the Rione Terra, that appeared like a medieval village, with a drawbridge at the entrance to the
 1615 cliff. The same context was depicted in the 11th century by the Arab geographer *Idrisi* in his *Opus*
 1616 *Geographicum*, describing Pozzuoli as a "castle" (Varriale, 2004).

1617 In the 12th century subsidence was still active. A writing deriving from an account of Benjamin ben Yonah
 1618 de Tudela who, visiting the Jewish communities of the Mediterranean, passing through Pozzuoli, described:
 1619 *turres et fora in aqua demersa quae in media quondam fuerant* (Russo Mailer C. 1979, Caruso 2004). The
 1620 Pozzuoli district continued to subside in the 13th century, as can be deduced from an account written in 1251
 1621 by the historian Niccolò Jamsilla (*Historia de rebus gestis Frederici II imperatoris ejusque filorum*
 1622 *Corradiet Manfredi Apuliaeet Siciliae regnum*) describes the places between Agnano and Pozzuoli as
 1623 follows: ...*videlicet Putheolum mari mantibusque inaccessibilius circumquaque conclusum*...(Fuiano
 1624 1951).

1625 In essence, what was observed by the Arab geographer Idris in the 11th century, was also written by the
 1626 historian Jamsilla in 1251, confirming that Rione Terra "was *an unapproachable mountain completely*

1627 *surrounded by the sea*". This highlights that, over more than 3 centuries, the sea level rose due to subsidence
1628 of the tuffaceous walls of the Rione Terra.

1629

1630 **8** – Further eyewitness accounts from by Boccacio, who lived in Naples between 1327 and 1341, reported that
1631 a fisherman's wharf in the Bay of Pozzuoli became completely submerged (Mancusi, 1987). This document
1632 supports the description of the lower part of the city being completely submerged.

1633

1634 **9-10** – A gouache from 1430, known as *Bagno del Cantariello*, part of the famous Balneis Puteolanis of the
1635 Edinburgh Codex (Di Bonito & Giamminelli, 1992) indicates the complete submergence of the 4th floor of
1636 the Serapeum by at least 10 meters. (Fig. 7). This context is supported by a description from 1441 indicating
1637 that in 1441 *"the sea covered the littoral plain, today called Starza"* (De Jorio, 1820; Dvorak and
1638 Mastrolorenzo, 1991) (see Fig. 8).

1639 For a more precise description of this morphological context, it is useful to refer to the excavation of the
1640 Serapeum carried out in 1750, when this monument was freed from the blanket of sediments that buried it (see
1641 Fig. 12), made up of approximately 8 m of filling sediments, plus two meters of deposits from the pyroclastic
1642 flow of the M. Nuovo eruption. By replacing the latter materials with the approximately 2 m blade of sea water
1643 in the 1430 scenario (Fig. 7c), we arrive at the landscape picture in Fig. 7a, exemplified in Fig. 8d.

1644

1645 **11 -13** – These points on the curve were obtained by determining the extent of subsidence from 1580 to
1646 1753, that is, respectively, the date on which the seismic phase after the 1538 eruption ended, and the date on
1647 which the excavation work on the Serapeum ended. The subsidence was inferred by comparing the
1648 engraving of 1584 by Cartaro, representing the Caligoliano pier (Fig.10a), and the engraving of the two
1649 testimonies: a) that of the Caligoliano pier reproduced in the Cartaro engraving of 1584 (fig. 10a) compared
1650 with its remains represented in an engraving from 1750 (fig. 10b), and with the same remains reported, more
1651 in detail, in another engraving of the middle 18th century (Fig. 10c): both the engraving dates were reported
1652 by Maiuri (1934). A further constraint about the extent of subsidence in the mentioned period comes from
1653 the level of the 4th floor of the Serapeum, which was found at 0.7 m asl during the excavations of 1750-1753
1654 (point 13) and was raised above sea level by 6-7m until 1580. The subsidence was then estimated at 5m.

1655 **14** – measurement by Niccolini at the end of 18th century (0.3 m asl).

1656 **15 - 18** – precise measurements of the height of the 4th floor, repeated by Lyell, Babbage and others until the
1657 end of the century (Parascandola, 1947).

1658 The following points in the diagram, from the beginning of 1900 to 1950, were detected with precision
1659 instruments from the Military Geographic Institute (IGM), while the more recent ones (since 2000) were
1660 measured using GPS methodology.

1661

Appendix 3 - Comparing past and recent earthquakes: from intensity to magnitude

To better compare the past **earthquakes** with the recent and present-day seismicity recorded at Campi Flegrei we must convert intensities in magnitude. In Fig. 19, we present a tentative correlation between the epicentral intensity (I_o) and the magnitude (M_L). Choosing the correct relation between I_o and M_L is not straightforward, particularly in this case involving peculiar volcano-tectonic earthquakes. Nonetheless, it is important to establish such a relation to compare the seismicity observed during the 1430-1582 period, as inferred by Guidoboni and Cucciarelli (2011), with the seismicity experienced during the recent unrests. To determine the I_o - M_L relation, we are confident that, despite the availability of several formulas in the literature, the best approach is to consider a precise geographical and seismotectonic context, especially in a volcanic setting. Different features allow to discriminate between volcanic and tectonic earthquakes, which suggests caution in using correlations derived from tectonic areas for volcanic earthquakes, and vice versa (Milana et al., 2010). In order to build a realistic relation between seismic intensity and magnitude in this area, we utilized the computed intensities of two earthquakes that occurred in the Campi Flegrei region in 1983 (Branno et al., 1984; Marturano et al., 1988; Milana et al., 2010; Charlton et al., 2020), during the previous unrest of 1982-1984 (Troise et al., 2019). Additionally, we considered a $M=5.0$ earthquake that occurred in the similar volcanic area of Colli Albani (Sabetta and Paciello, 1995). The $M=4.0$ earthquake occurred on October 4, 1983, at Campi Flegrei, was found to have a maximum intensity $I_o=VII$ (Branno et al., 1984; Marturano et al., 1988). An earthquake of magnitude $M=3.5$, which occurred in the same swarm on October 4, 1983, was found to have a maximum intensity $I_o=V$ (Fig. 19: Marturano et al., 1988). Furthermore, Sabetta and Pugliese (1995) reported an earthquake of $M=5.0$, with a maximum magnitude $I_o=VIII$. These correlations between intensity and magnitude were utilized to assign realistic magnitude values to the macroseismic intensities deduced from the analysis of historical seismicity (Guidoboni and Cucciarelli, 2011), as shown in Fig. 19. They were also used to transform the magnitude of earthquakes associated with recent unrest phases into macroseismic intensities, as we will discuss later.